Please do not adjust margins

Journal Name

ARTICLE

Dye Aggregation in Dye-Sensitized Solar Cells

Lei Zhang[ab] and Jacqueline M. Cole[*cdef]

Received 00th January 20xx,
Accepted 00th January 20xx

DOI: 10.1039/x0xx00000x

www.rsc.org/

Dye aggregation dictates structural and optoelectronic properties of photoelectrodes in dye-sensitized solar cells (DSSCs), thereby playing an essential role in their photovoltaic performance. It is therefore important to understand this molecular phenomenon so that dye aggregation can be suitably controlled in DSSC devices. Accordingly, this review presents the molecular origins of dye aggregation, manifestations of hypsochromic (H) and bathochromic (J) dye aggregation in DSSCs, a classification of the molecular factors that cause this aggregation, and ways by which dye aggregation can be suppressed in cases where it is undesirable. To this end, a classification of molecular engineering methods that are being used in order to better understand and control dye aggregation is described. The review concludes with a broader outlook on how molecular aggregation in chromophores can similarly effect a wider range of optoelectronic phenomena.

Lei Zhang received his PhD in Natural Science (Physics) in 2015 from the University of Cambridge. Prior to this, he earned his BS from Nanyang Technological University Singapore and MSc from Imperial College London. He joined the School of Physics and Optoelectronic Engineering at Nanjing University of Information Science and Technology (NUIST) in 2015 and is a faculty member in the Department of Applied Physics. His research interests include theoretical and experimental aspects of structure-properties relationships of functional molecules and their interfaces.

Jacqueline Cole is Head of Molecular Engineering at the University of Cambridge, a joint initiative between the Departments of Physics and Chemical Engineering and Biotechnology, in partnership with STFC Rutherford Appleton Laboratory. Jacqui designs new materials for energy and environmental applications. She holds the 1851 Royal Commission 2014 Fellowship in Design. Other professional recognition includes: Fulbright Award (2013-4); Royal Society University Research Fellowship (2001-11); Royal Society of Chemistry SAC Silver Medal (2009); Royal Society Brian Mercer Feasibility Award (2007); Franco-British Science prize (2006); Junior and Senior Research Fellowships, St Catharine's College, Cambridge (1999-2009); British Crystallographic Association Chemical Crystallography Prize (2000).

1. Introduction

The transparent and low-cost nature of dye-sensitized solar cells (DSSCs) affords them niche applications as solar-powered windows.[1,2] Such 'smart windows' herald exciting prospects for creating energy-sustainable buildings for future cities. The dye is a particularly important material component of the DSSC, as it carries out two different functions: light-harvesting and initiating the electrical current in the solar cell.[3,4] These two functions occur sequentially, whereby the dye molecule initially absorbs light from the sun, thus generating a photo-excited dye which, in turn, injects an electron into the conduction band of the semiconductor (usually TiO_2) onto which the dye is adsorbed. Since this dye/semiconductor composite comprises

[a.] *Jiangsu Key Laboratory for Optoelectronic Detection of Atmosphere and Ocean, Nanjing University of Information Science & Technology, Nanjing 210044, China*
[b.] *Department of Applied Physics, School of Physics and Optoelectronic Engineering, Nanjing University of Information Science & Technology, Nanjing 210044, China*
[c.] *Cavendish Laboratory, University of Cambridge, J. J. Thomson Avenue, Cambridge, CB3 0HE, UK. E-mail: jmc61@cam.ac.uk*
[d.] *Argonne National Laboratory, 9700 S Cass Avenue, Argonne, IL 60439, USA*
[e.] *ISIS Neutron and Muon Facility, STFC Rutherford Appleton Laboratory, Harwell Science and Innovation Campus, Didcot, OX11 0QX, UK.*
[f.] *Department of Chemical Engineering and Biotechnology, University of Cambridge, West Cambridge Site, Philippa Fawcett Drive, Cambridge, CB3 0AS, UK.*

This journal is © The Royal Society of Chemistry 20xx

Please do not adjust margins

Please do not adjust margins

the working electrode of the solar cell, this electron-injection process initiates the electrical current in the photovoltaic device. The ways dye molecules are adsorbed onto the TiO_2 surface thereby controls the performance of the DSSC. One might naively consider dye molecules to align neatly on the TiO_2 surface. However, experimental findings testify to a much more complicated scene. Dyes orient on the TiO_2 surface in different ways,[5] and dye···dye separation on this surface varies, presumably due to dye-specific steric and electronic factors. Dye molecules may also aggregate, either prior to adsorption onto the TiO_2 surface during the DSSC fabrication process, or thereafter.[6,7]

This dye aggregation can severely disrupt the function of a DSSC device; as such, its molecular origins need to be understood and controlled in order to mitigate any harmful effects it may have on the photovoltaic output of the DSSC.[3,8] Yet, such understanding is difficult to achieve, given that dye aggregation is very common and complex on the molecular level. While many individual reports on dye aggregation exist, there appears to be no coherent piece that aims to collate the important studies and reviews of this area within a single paper. This review on dye aggregation in DSSCs has been written to help to close this gap.

This review will begin with an introduction to DSSCs, whereby the chemical processes associated with the operational mechanism in DSSCs will be described, with a focus on the molecular factors that influence the function of the DSSC working electrode, which comprises a dye···TiO_2 interface. Dye aggregation will be introduced as one of these factors, and the scope of the review will then be defined in this respect. To that end, the basic concepts of H- and J-aggregation will be described, in the context of molecular exciton theory. These effects of dye aggregation on DSSCs will then be exemplified by reviewing experimental and computational case studies. Examples will be given on how dye aggregation can affect the photovoltaic DSSC performance in a beneficial, detrimental, or auxiliary manner. Molecular factors that govern dye aggregation will be classified, and the ways molecular engineering methods can be used to mitigate dye aggregation in DSSCs, to improve device performance, will be illustrated. Finally, the review considers how molecular aggregation of chromophores can also affect other optoelectronic phenomena such as non-linear optical activity or electron mobility in organic transistors.

1.1. Operational mechanism of DSSCs

A DSSC consists in essence of a photo-anode and a photo–cathode that are connected via an electrolyte (Figure 1). In this setup, the photo-anode comprises dye molecules immobilized on a semiconductor oxide substrate, which is responsible for the absorption of light and the photon-to-electron conversion. The performance of a DSSC is characterized by the overall device performance conversion efficiency (η), short-circuit current density (J_{sc}), open-circuit voltage (V_{oc}), fill factor (*FF*), and incident-photon-to-current conversion efficiency (*IPCE*).

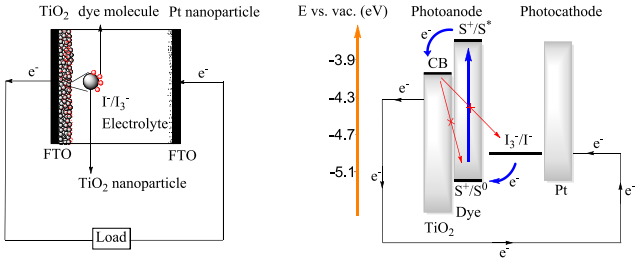

Figure 1 Schematic structure of a DSSC, consisting of a photo-anode, electrolyte, and a photo-cathode (left); charge-transfer steps involved in a DSSC (right). Blue arrows indicate normal steps involved in a working DSSC, i.e., light absorption, dye-to-TiO_2 charge transfer, and regeneration of the dye by the electrolyte. Red arrows indicate parasitic charge transfer from injected dyes to the oxidized molecule or the electrolyte.

1.1.1. Overall device performance conversion efficiency (η)

The overall power conversion efficiency (η) of a photovoltaic device is one of the most important parameters in solar cell research, which is defined by the short-circuit photocurrent density (J_{sc}), the open-circuit photovoltage (V_{oc}), the fill factor (*FF*), and the incident light power (P_{in}):

$$\eta = \frac{J_{SC} V_{OC} FF}{P_{in}} \qquad (1)$$

1.1.2. Short-circuit current density (J_{sc})

The short-circuit current density (J_{sc}) is the current density measured when no external bias is applied. J_{sc} is strongly influenced by the light absorption of the dye molecules, their intramolecular charge transfer, and the interfacial charge transfer from the dye molecules to the semiconductor substrate.

1.1.3. Open-circuit voltage (V_{oc})

V_{oc} is the difference between the redox level of the electrolyte and the quasi-Fermi level of the semiconductor. V_{oc} is affected by the concentration of electrons in the conduction band (CB) of the semiconductor and the magnitude of electron recombination from the injected dyes to the oxidized electrolyte:[9,10]

$$V_{OC} = \frac{E_{CB}}{q} + \frac{kT}{q}\ln\left(\frac{n}{N_{CB}}\right) - \frac{E_{redox}}{q} \qquad (2)$$

where n is the number of electrons in the semiconductor, N_{CB} the effective density of states in the semiconductor, E_{CB} the energy level of the bottom of the CB of the semiconductor, E_{redox} the energy level of the electrolyte, and q the unit charge.

1.1.4. Fill factor (FF)

Moreover, η is strongly affected by the fill factor (*FF*), which is defined by the ratio of the maximum power of the solar cell to the product of J_{sc} and V_{oc}. It is therefore essentially a measure of the quality of a solar cell. As such, *FF* varies with different fabrication methods, characterization conditions, and the series resistance.[11]

This journal is © The Royal Society of Chemistry 20xx

Please do not adjust margins

Please do not adjust margins

1.1.5. Incident photon-to-current conversion efficiency (IPCE)

The incident photon-to-current conversion efficiency (*IPCE*) is another fundamental indicator for the performance of a solar cell.[2] It is defined as the ratio between the photocurrent density produced in the external circuit under monochromatic illumination of the cell and the incident photon flux:

$$IPCE = \frac{J_{SC}(\lambda)}{q\Phi(\lambda)} \quad (3)$$

The *IPCE* is closely related to the light-harvesting efficiency and comprises the following contributions:

$$IPCE(\lambda) = LHE(\lambda) \times \varphi_{inj}(\lambda) \times \varphi_{reg} \times \eta_{CC}(\lambda) = LHE(\lambda) \times APCE(\lambda) \quad (4)$$

where *LHE* is the light-harvesting efficiency, φ_{nj} the quantum yield for electron injection, φ_{reg} the quantum yield for dye regeneration, and η_{cc} the charge-collection efficiency. The product of φ_{inj}, φ_{reg}, and η_{cc} is called absorbed-photon-to-current-conversion efficiency (*APCE)*, which characterizes the efficiency of the conversion of the absorbed photons into electrical current.[12]

1.2. Molecular factors that control DSSC function

The molecular origins of DSSC function concern a range of factors that are associated with the dye. Such factors concern the molecular constitution of the dye molecule, the susceptibility of the dye to its solution environment during the dye sensitization process that creates the DSSC working electrode, and the nature of the dye···TiO_2 interface that comprises this electrode. These three states of the dye need to be considered when judging the prospects of a dye for DSSC application. For example, the chemical nature of the dye will influence DSSC function via its molecular shape and size, the nature and extent of intramolecular charge transfer that pervades the dye molecule, the type of substituents that the dye may possess (e.g. long alkyl chains that act as hydrophobic groups), and the nature of the chemical substituent that acts as the anchoring point for the dye to adsorb onto the surface of the TiO_2 semiconductor.[13] The dye is dissolved into a solution in order to fabricate the DSSC working electrode, whereby a μm-thick layer of TiO_2 on a substrate of transparent conducting oxide glass is submerged into this solution for a sufficient time that the dye molecules have chance to adsorb onto the TiO_2 surface. A range of factors may influence this dye sensitization process, including the dye concentration, temperature and pH value of this solution, the choice of solvent, the sensitization time, and any additives that may be present in the solution. The dye···TiO_2 interface that comprises the resulting DSSC working electrode is in turn affected by the nature of its molecular environment. This can influence the charge characteristics of its operation in terms of electron injection, electron recombination and dye regeneration and such charge effects can in turn affect device stability.

The molecular aggregation characteristics of a dye are in fact influenced by all three states of a DSSC dye. The chemical nature of the dye (e.g. its polarity and types of substituents) will influence its innate ability to interact with another molecule of its own. The experimental conditions of the fabrication process will determine how many dye molecules can interact with each other, or with another type of chemical (e.g. solvent, additive), or indeed be inhibited from interaction. The dye···TiO_2 interfacial structure is assumed to feature a monolayer of homogeneously spaced dyes, but the clustering of dyes could negate this monolayer structure if present in the lateral direction, while dye aggregation in the longitudinal direction would void the homogeneous dye distribution. A dye that binds on top of another dye instead of the TiO_2 surface will negate its own photovoltaic function, as it will not be able to interact with the TiO_2 surface to undergo electron injection, while also preventing the electrolyte ion from reaching the cognate dye on the TiO_2 surface to afford it electron regeneration. Meanwhile, a dye molecule that binds to the TiO_2 surface too close to another dye molecule on that surface stands to result in dye···dye interactions, which could affect their charge characteristics in a beneficial or deleterious fashion.

The nature and extent of dye aggregation in DSSCs therefore needs to be understood in good detail if its effect on photovoltaic function is to be discerned. Fortunately, molecular exciton theory helps explain how dyes aggregate in solution or on a solid support, and how this impacts on their energetics that can be detected as solvatochromic shifts in UV/vis absorption spectra. These shifts may be hypsochromic or bathochromic according to the bimodal classification of dye clustering as H- or J-aggregates.

2. Dye aggregation in DSSC dyes

2.1 H- and J-aggregates as explained by molecular exciton theory

2.1.1 Energy-level description of molecular exciton theory

The photophysical behavior of organic molecules used for many technological applications such as photovoltaics, sensors, and light-emitting diodes is governed by the structure and dynamics of their low-lying electronic states. These excited electronic states, which are collectively called excitons, and can be thought of as mobile quasiparticles that carry energy. Excitons can be described in terms of a site Hamiltonian, whereby each site has two molecular orbitals. The electronic states of molecules change as they assemble to form aggregates.[14] The optical properties of dye aggregates can be described by Kasha's molecular exciton theory,[15] which describes a resonance splitting of the excited state composite molecular energy levels, which are non-degenerate in the individual molecule or light-absorbing unit. The molecular exciton theory states that when two monomeric dyes (1 and 2) are interacting to form a dispersive dimer, coupling phenomena lead to excited state splitting,[15–17] whereby the energy of the excited dimer becomes either:

$$E^{\dagger\prime} = E_1^{\dagger} + E_2 + \int\int \psi_1^{\dagger}\psi_2(V_{12})\psi_1^{\dagger}\psi_2 \mathrm{d}\tau_1 \mathrm{d}\tau_2 + \int\int \psi_1^{\dagger}\psi_2(V_{12})\psi_1\psi_2^{\dagger}\mathrm{d}\tau_1\mathrm{d}\tau_2 \quad (5)$$

or:

Please do not adjust margins

Please do not adjust margins

$$E^{\dagger\prime\prime} = E_1^{\dagger} + E_2 + \int\int \psi_1^{\dagger}\psi_2(V_{12})\psi_1^{\dagger}\psi_2 d\tau_1 d\tau_2 - \int\int \psi_1^{\dagger}\psi_2(V_{12})\psi_1\psi_2^{\dagger} d\tau_1 d\tau_2 \quad (6)$$

wherein † denotes the excited state, E_1 and E_2 the ground state energy of molecule 1 and molecule 2, respectively, while V_{12} is the intermolecular perturbation potential. Figure 2 schematically represents the energy splitting due to molecular exciton theory. The last term in equations (5) and (6) is the so-called exciton-splitting term, which represents the interaction energy due to the exchange of excitation energy between molecules 1 and 2:

$$\xi = \int\int \psi_1^{\dagger}\psi_2(V_{12})\psi_1\psi_2^{\dagger} d\tau_1 d\tau_2 \quad (7)$$

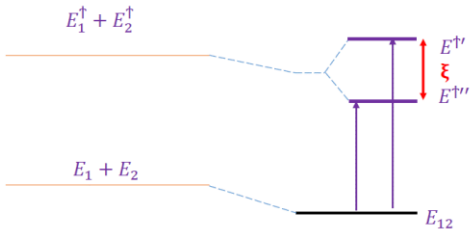

Figure 2 Schematic representation of the molecular exciton theory. The left side represents the energy of the monomer, while the right side represents the energy of the dimer.

2.1.2 Relating energy levels to dye-aggregated structures

The excitation energy of a dye dimer depends on the arrangement of the molecular dipole moments. H-aggregates (termed after the concomitant hypsochromic shift of the absorption spectra) or J-aggregates (named after their co-discoverer Jelley) are obtained for face-to-face or edge-to-edge arrangements of the dipole moments (Figure 3).[14,18]

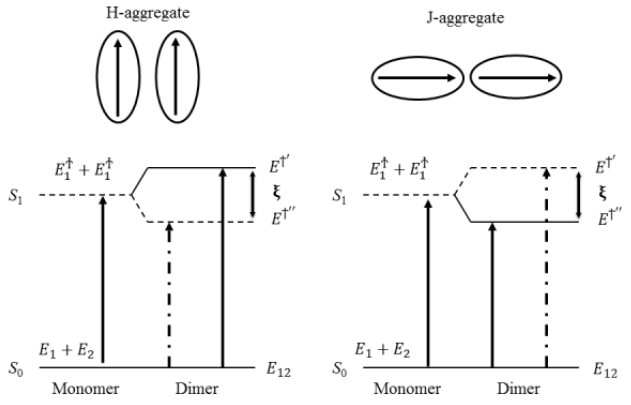

Figure 3 Simplified schematic of exciton theory to explain the different absorption behaviors of H- and J-aggregates. The dotted lines help to explain the relative populations that relate the molecular alignment to the energies of the exciton band.

The face-to-face alignment of molecules results in a hypsochromic absorption shift, since the difference between the molecular dipole moment of the monomer and that of its aggregate is very small. The associated transition dipole moment is thus essentially negligible, resulting in a fast energy relaxation of absorbed photons from the exciton band to the ground state. Consequently, the lower energy state in this exciton band is barely populated, while the ephemeral population of the upper energy state renders a low quantum yield. This ephemeral population is nonetheless detectable in UV/vis absorption spectroscopy as an absorption band, whose peak is high-energy-shifted relative to the peak maxima that corresponds to the monomer. This is the hypsochromic shift that is assigned to H-aggregates of the monomeric species of the sample under investigation, providing evidence that face-to-face molecular aggregates have formed.

In contrast, the edge-to-edge alignment of molecules generally creates aggregates whose dipole moment is significantly enhanced relative to that of the monomeric species, since molecules tend to align in a head-to-tail fashion owing to attractive forces of a polar molecule (such as a dye). This large difference in the molecular dipolar moment of the monomer and that of the aggregate results in a large transition dipole moment upon photon absorption. The lower level of the exciton band is thus stabilized such that a large population builds up in this state. Accordingly, an optical band of lower energy than that of the monomeric species is created from the formation of edge-to-edge aggregates, i.e., a bathochromic shift is observed in the UV/vis absorption spectrum that is assigned to J-aggregates. This band has a high quantum yield since it is associated with a highly populated exciton state.

This description of molecular exciton theory is most easily envisaged when dimers form in one of these two contrasting aggregate configurations. Aggregates that align somewhere in between these extremes of face-to-face or edge-to-edge molecular alignment are classified as H- or J-aggregates depending on whether the angle, α, between the transition dipole moment and the long axis of the aggregate that forms is higher or lower than $\tan^{-1}(\sqrt{2})$, i.e., 54.7°. Aggregates that contain more than two species will naturally generate exciton bands with more levels. The exciton bandwidth of an aggregate is determined using the angle, α, together with the angle between the transition dipole moments of neighboring molecules, the distances between molecules, and the number of interacting molecules in the aggregate.

2.2 H- and J-aggregates of DSSC dyes in the context of molecular exciton theory

H- or J-aggregates of dyes can form during the sensitization process of DSSC device fabrication, where the dyes exist in solution, or once the dye has adsorbed onto the TiO_2 to create a solid dye···TiO_2 interfacial structure that comprises the DSSC working electrode. Dye aggregation may present in neither, either, or both of the two different states, the nature and extent of which will vary according to the chemical nature of the dye or its local environment.

2.2.1 H- and J-aggregates of dyes in solution during the DSSC fabrication process

The molecular orientation preferences of dyes in solution are void of the physical restrictions of a solid support structure that constrains the dye orientation once the dye···TiO_2 interface has

This journal is © The Royal Society of Chemistry 20xx

Please do not adjust margins

Please do not adjust margins

formed. Dye molecules in solution are nonetheless susceptible to their local environment.

2.2.1.1. Molecular aggregation of dyes in solution caused by dye self-interaction.

This local environment could pertain to the dye itself, whereby a sufficiently high dye concentration could easily result in the formation of aggregates due to dye self-interaction. The pH value and temperature of the solution will influence the polarity of the dye molecules and its solubility, respectively, which in turn will impact on the exact concentration required for such aggregation. The choice of solvent will also affect the solubility of the dye in solution, as could the presence of any additives in the solution. The type of aggregate that forms owing to dye self-interaction will naturally be dye specific. A few examples of H- or J-aggregation in DSSC dyes caused by dye self-interaction are now given.

Simple face-to-face and edge-to-edge aggregation forms owing to the dyes interacting with each other. Therefore, the total concentration is one of the prime factors affecting dye aggregation. For example, benzothiazole-based dyes **1** and **2** with similar backbone structures can self-aggregate, whereby **1** exhibits H-aggregation, while **2** displays J-aggregation in solution. Dye aggregation in solution and the subsequently observed aggregates and dynamics have been analyzed particularly in aqueous solutions,[19–23] as these play an essential role in the textile and coloration industries.

In addition, temperature changes affect dye aggregation at a constant concentration, whereby increases in temperature usually help to dissolve dye aggregates. For example, there is a strong temperature dependence of the H-aggregation for benzothiazole-based dye, **3**, where the dissociation constant increases by two orders of magnitude when the temperature is raised from 10 to 80 °C.[24]

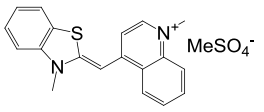

1

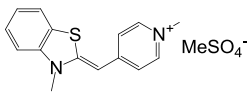

2

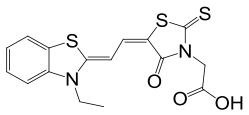

3

In some cases, molecular aggregation can be controlled or manipulated via the pH value. For example, dissolving azo dye **4** (Solophenyl red 3BL) in highly acidic aqueous solutions leads to J-aggregates.[25] Neutral pH leads to monomer formation of porphyrin dye **5**; decreasing pH leads to preferential H-aggregates and further acidification of the solution leads to J-aggregates (Figure 4).[26]

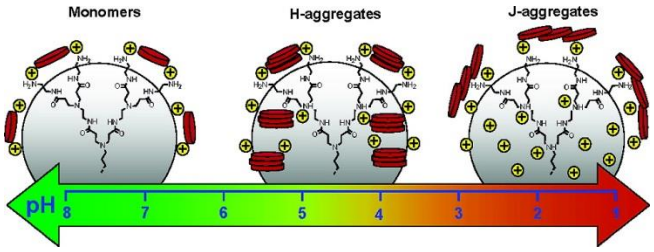

Figure 4 The formation of monomers, H-aggregates, and J-aggregates of **5** in response to the changes in pH.[26] The monomers and aggregates are highlighted in red. Reproduced with permission from reference 26. Copyright ACS (2005)

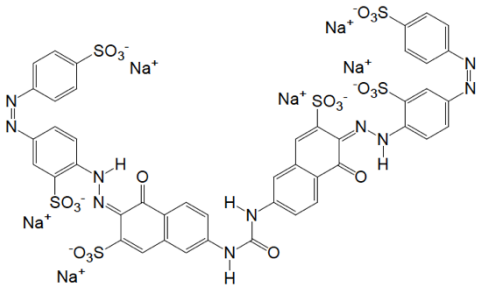

4

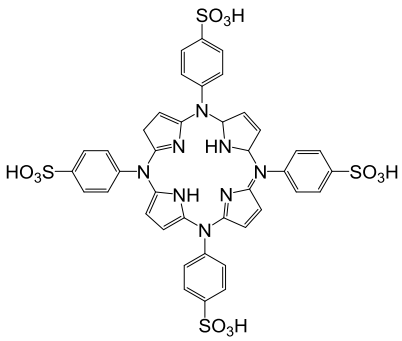

5

Furthermore, the solvent composition affects dye polarization and thus dye aggregation: dyes are usually fully solvated, i.e., monomeric in good solvents, while they aggregate in solvents where they exhibit poor solubility.[27,28] The dimeric aggregation of the *trans*-azobenzene dye **6** affects its optical properties, e.g. its photoisomerization in aqueous solution, which decelerates upon aggregation.[19] In addition, optically active J-aggregates of cyanine dye **7** in aqueous solution can act as a chirality sensor, as the J-aggregates are sensitive to chiral additives.[29] Benzothiazole-based dye **3** exhibits a hypsochromically shifted absorption band in water, which has been assigned to a dimer.[24] The aggregation phenomena of a donor–acceptor tetrathiafulvalene dye **8** and its derivatives have been studied via optical absorption and electron spin resonance spectra in solution, which revealed the presence of homoleptic dimers and mixed-valence dimers. The intramolecular electron transfer within the dye reciprocally influences the intermolecular charge transfer occurring in a dimer.[30] The aforementioned examples should be considered as merely representative, since control over H- and J-aggregation has been examined for a large variety of dyes in solution,[20–22,31–45] and is very dye specific.

Please do not adjust margins

Please do not adjust margins

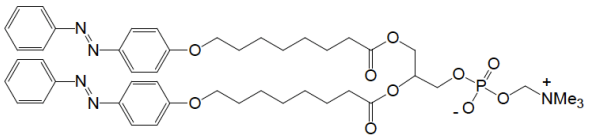

6

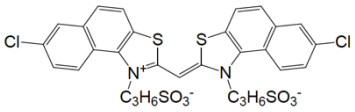

7

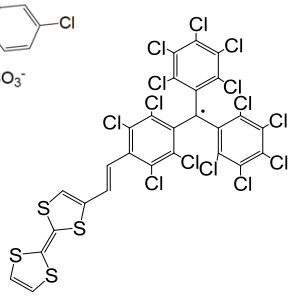

8

The dye self-interaction links directly with molecular exciton theory via the mutual orientation of each dye. Coumarin dye **9** shows dyes self-interacting in a specific mutual orientation, as the coumarin dye is prone to aggregation in solution, whereby its different aggregation phases depend on the polarity of the solvent. Based on UV/vis absorption profiles and crystal structures, the presence of monomers, dimers, and higher-order J-aggregates has been proposed (Figure 5).[46]

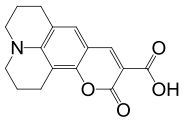

9

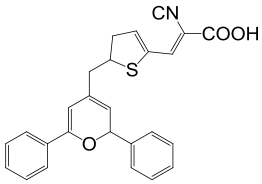

10

The arrangement of the dye aggregates affects their transition dipole moment,[47] as well as the light-absorption and emission properties.[47] For example, the results of density functional theory (DFT) calculations have shown that the relative angles between molecular dipoles (0° or 180°) may affect the light-absorption properties of the DSSC-active dye **10**.[16]

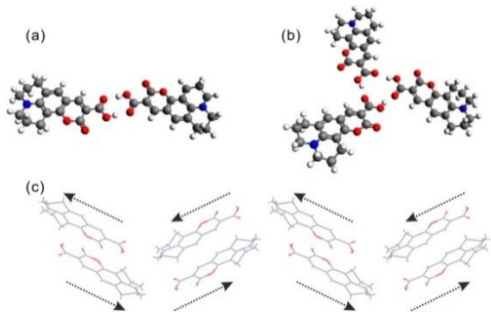

Figure 5 (a) Dimeric (b) trimeric, and (c) high-order aggregate models of **9** in solution.[46] Reproduced with permission from reference 46. Copyright ACS (2013).

2.2.1.2 Molecular aggregation of dyes in solution that has been influenced by dyes interacting with another type of molecule or ion

The choice of solvent or the presence of additives to a dye solution were described in the last section as factors that could *implicitly* affect how dyes self-interact. However, a solvent or additive could also interact *explicitly* with the dye molecules and such interactions could, in turn, affect how dyes aggregate. A representative selection of examples that illustrate these explicit influences is now given.

Explicit solvent molecules can influence the dye aggregation in solvents. For example, an external solvent molecule can form an intermolecular hydrogen bond with azo dye **11**, therefore tuning the solvatochromism through the manipulation of aggregation (Figure 6).[48]

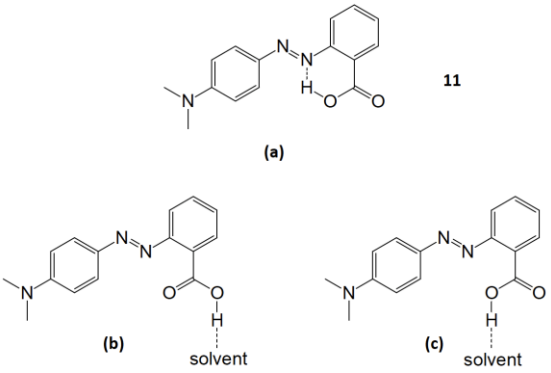

Figure 6 Hydrogen bonds in azo dye **11**: (a) intramolecular hydrogen bond without external solvent molecules; (b,c) intermolecular hydrogen bonds with an external solvent molecules.[48] Reproduced with permission from reference 48. Copyright ACS (2013).

Co-adsorbents and co-sensitizers could likewise influence the aggregation of dyes in solution. For example, additives such as polyanion residues shift the monomer/dimer equilibrium of benzothiazole-based dye **12** and its derivatives[49] towards H-aggregates, and reduce the fluorescence intensity at low dye loadings.[50] Upon addition of metal ions, benzothiazole-based dye, **13,** forms J-aggregates in aqueous solution, whereby the rate of aggregation depends on the nature of the metal ion and the dye, as well as on the temperature.[51]

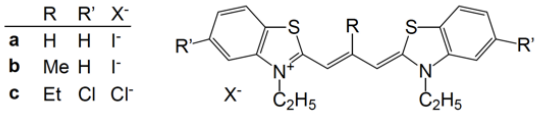

12

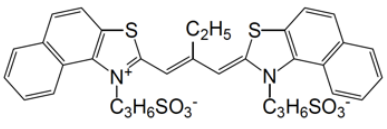

$C_5H_5NH^+$

This journal is © The Royal Society of Chemistry 20xx

Please do not adjust margins

Please do not adjust margins

2.2.2. H- and J-aggregates of dyes that form at the dye···TiO_2 interface

The sensitization process immobilizes dye molecules on the TiO_2 surface, most typically as a self-assembled monolayer (SAM). This SAM can nonetheless consist of dye monomers or aggregates.[52,53] Aggregates form when the dye monomers become too close to each other, either in lateral or longitudinal direction relative to the TiO_2 surface. In longitudinal direction, dye molecules may clump together in certain parts of the TiO_2 surface, thereby precluding a homogeneous distribution of dyes. Alternatively, a homogeneous SAM of dyes may form wherein all dye molecules lie so close to each other that the entire SAM comprises an aggregate. In the lateral projection, dye molecules that are part of the SAM may form aggregates by interacting with other dye molecules via the part of their molecule that protrudes away from the TiO_2 surface. These aggregates may form via a dye molecule landing on top of the SAM, or via a dye molecule that is part of the SAM forming aggregates with other dye molecules before it lands onto the TiO_2 surface, during the fabrication process. Figure 7 illustrates these types of scenarios, which involve select dye molecules clumping together, or clustering on mass, on the TiO_2 surface, or landing on top of a dye monolayer.

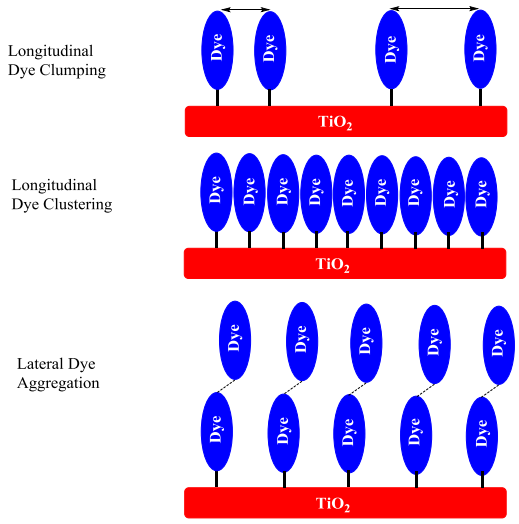

Figure 7 Three types of dye aggregation forming on the surface of TiO_2 semiconductor substrates (longitudinal dye clumping, dye clustering; lateral dye aggregation).

2.2.2.1 H- and J-aggregates of dyes that form within the monolayer of dyes on the TiO_2 surface

These types of aggregates largely form during the dye sensitization process, as the SAM of dye molecules takes shape on the TiO_2 surface, since the dye distribution is thereafter considered to be set. Face-to-face aggregates are the most likely to form under these circumstances since dyes tend to line up in this type of orientation with each other in an SAM. Representative examples of these types of dye aggregates have been given by Feng *et al.*,[54-56] who used time-dependent density functional theory to model face-to-face aggregation in two DSSC dyes (**14** and **15**). Each dye forms dimers on the TiO_2 surface via intermolecular $\pi\cdots\pi$ interactions, but the associated dye···dye intermolecular electronic coupling in **15** is only 10% of that of **14**. Feng *et al.*[54] have shown that this is due to the presence of a diphenylquinoxaline anti-aggregation unit between the donor and acceptor groups of **15**.

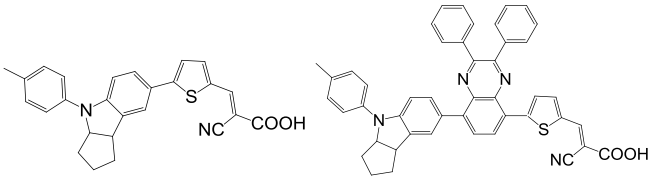

14 **15**

2.2.2.2 H- and J-aggregates of dyes that form on top of the monolayer of dyes on the TiO_2 surface

These types of aggregates may originate from one of several scenarios, e.g. when excess dye molecules are present during the sensitization such that they add to the top of an already saturated SAM of dyes on TiO_2; and in doing so, they interact in a fashion that renders them bound to each other. Alternatively, the dyes may reach the TiO_2 surface in an already aggregated form, wherein the binding strength of the aggregate complex is too strong for it to break apart, even as a consequence of one or more of the dyes in this aggregate adsorbing onto the TiO_2 surface as part of its SAM of dyes. Either way, these dyes are likely to aggregate in an edge-to-edge fashion since it is the edge of the dye on the SAM that is available for the formation of intermolecular interactions.

Several examples of these types of aggregates have been demonstrated via imaging studies of dyes on TiO_2 surfaces. Scanning tunneling microscopy (STM) measurements revealed molecular aggregates of the Black Dye (N749, **16**) on the rutile TiO_2 (110) surface.[57] Dye aggregation lateral to this TiO_2 surface was specifically observed and quantified, indicating that the Black Dye could stack up to three molecules high, even at low dye-sensitization times and concentrations. An Atomic Force Microscopy (AFM) study[58] showed that the dye Z907 (**17**), which is chemically similar to **16**, also forms aggregates lateral to the TiO_2 surface during the sensitization. The crucial difference between **17** and **16** is that the former features long alkyl chains; these enable **17** to stand upright on the TiO_2 surface, and the AFM images indicate that during certain periods of the sensitization process, stacks of **17** reach the height of two molecules.

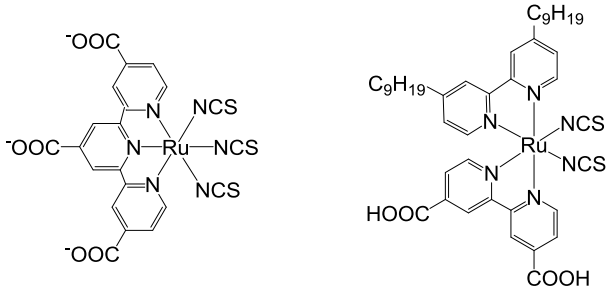

Please do not adjust margins

16 17

2.2.3 Energetic considerations of H- or J-aggregation

Notwithstanding the topological considerations of molecular exciton theory, the energetics associated with H- or J-aggregation of a dye are important indicators of solar-cell performance. For DSSC applications, H-aggregation is usually undesirable since the hypsochromic shift prevents the dye from absorbing in the longer wavelength region of the visible spectrum, as well as in the near infra-red (NIR) region, both of which constitute desirable parts of the solar spectrum. Moreover, for most optoelectronic devices it is more difficult to absorb photons in the longer-wavelength region of the visible spectrum relative to photons in the UV region. The band gap of semiconducting materials usually allows them to absorb photons in the former region, while narrower band gaps generally lead to an enhanced absorption of photons in the NIR region. Nevertheless, evidence has been presented that shows that H-aggregation may broaden UV/vis absorption spectra with respect to the monomeric form, thereby enhancing the light-harvesting and DSSC performance of the dyes.[59,60] Compared to H-aggregates, J-aggregates are universally beneficial for light absorption, and they have accordingly received substantially more attention.[61,62] Since the discovery of J-aggregates in the 1930s, intriguing insights into the operation of dye systems have been revealed, which have motivated research into custom-tailored dyes for specific applications.[62]

Many dyes employed for DSSC applications exhibit H-aggregation. For example, benzothiazole-based dye **3** displays H-aggregates upon sensitization of colloidal semiconductor particles.[24] Sensitization of nanocrystalline TiO_2 with benzoxazole-based dye **18** results in an absence of J-aggregates, and equal power conversion efficiencies (PCEs) were observed between the monomeric and the aggregated forms of **18**.[63] Polyene dyes including retinoic and carotenoic acids and their analogues form H-aggregates on TiO_2 substrates. The observed increase of the photocurrent upon lowering the concentration of the polyene dyes was ascribed to the suppression of aggregation at low concentrations.[64,65] Ionic dyes including acid orange 7 (**19**), crystal violet (**20**), and methylene blue (**21**) exhibit dye aggregation and a hypsochromic shift of their absorption bands upon deposition on TiO_2. H-aggregates of pyrogallol red (**22**) are able to inject electrons into the CB of the TiO_2 substrate.[66] A series of chalcogenorhodamine dyes (**23**) with phosphonic and carboxylic acid groups adsorb onto TiO_2 nanoparticles as mixtures of H-aggregates and monomers, which results in broadened absorption spectra. Anchoring on the surface via various functional groups affects the extent of H-aggregation minimally, while H-aggregation does not reduce the electron-injection yield or charge-collection efficiency of DSSCs containing chalcogenorhodamine dyes.[60] For dye **24**, time-resolved laser spectroscopy measurements revealed electron-injection rate constants of 0.21 ps^{-1} (monomers) and 0.07 ps^{-1} (H-aggregates), which demonstrate that H-aggregation retards the electron-injection rates. Moreover, a rate constant of 0.04-0.25 ps^{-1} can be observed for the energy transfer from the excited state of the monomers to the H-aggregates.[67] Azo dyes such as *para*-methyl (**25**) and *para*-ethyl red (**26**) exhibit substantial H-aggregation on TiO_2 substrates due to their azobenzene backbone, which is well-suited to engage in $\pi\cdots\pi$ interactions.[48,68–71] The phenothiazine-based dye **27** exhibits H-aggregation on TiO_2 films in DSSCs, and the aggregation can be modulated by the presence of thiophene and ethylenedioxythiophene.[72] Apart from its influence on electron injection, dye aggregation can significantly reduce photodegradation by pollutants adsorbed onto TiO_2; see for example the case of dyes **19**-**21** where their interaction with the photocatalyst is inhibited.[73]

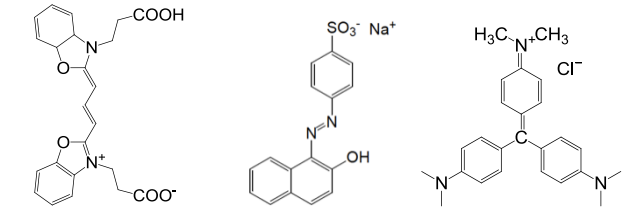

18 19 20

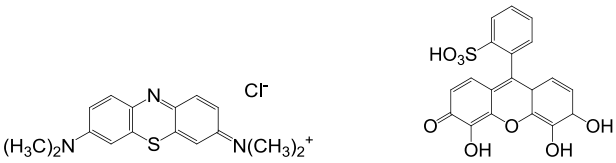

21 22

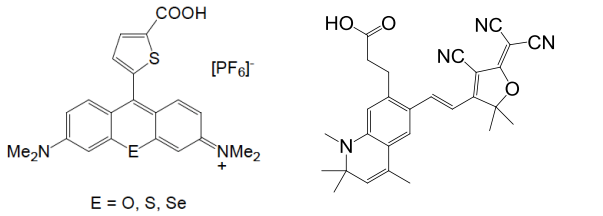

23 24

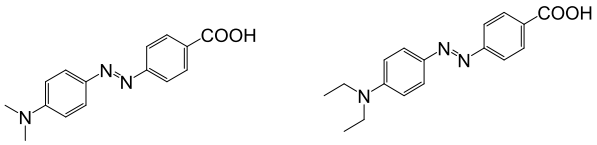

25 26

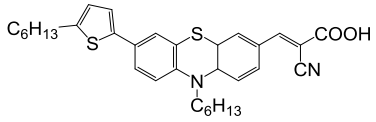

27

J-aggregation is better suited to enhance solar cell performance due to its effective capture of NIR photons, and various dyes form J-aggregates on semiconductor substrates. For example, the benzothiazole merocyanine dye **28** forms J-aggregates that differ in aggregate size.[74] Depositing porphyrin dye **29** onto a nanocrystalline TiO_2 film results in the formation of J-aggregates and a concomitant optical absorption at 420, 654, and 795 nm. Interestingly, these dyes show fluorescence on Al_2O_3 films,

This journal is © The Royal Society of Chemistry 20xx

while such fluorescence is not observed on TiO_2 particles.[75] Porphyrin dye **30** simultaneously forms H- and J-aggregates upon adsorption onto the interfaces of nanocrystalline TiO_2, whereby aggregation can be controlled by varying the electrolyte anion; in this case, J-type aggregates showed better solar cell efficiency than H-type aggregates.[76]

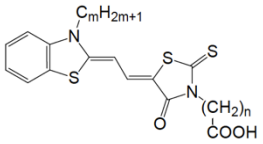

28

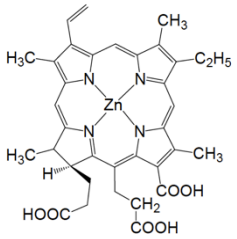

29

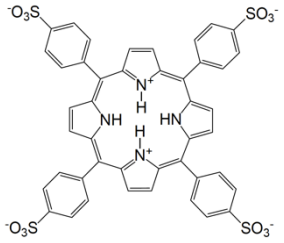

30

The exciton energy and charge transfer of J-aggregates of porphyrin dye **31** on TiO_2 have been analyzed by Verma and Ghosh.[31] Such porphyrin aggregates are formed by weak van der Waals, π···π, electrostatic, and hydrogen-bond interactions, and exhibit a nonradiative decay via intermediate vibronic states (S1 and S2). Due to their low-energy exciton states, J-aggregates receive energy from the porphyrin monomers that are not directly adsorbed on TiO_2 (Figure 8).[31]

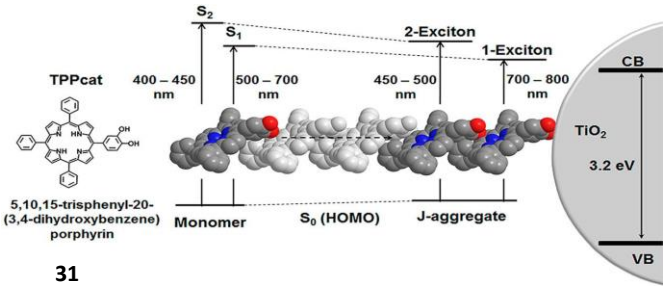

31

Figure 8 Diagram for the exciton energy and charge transfer in monomeric **31** and its J-aggregates on TiO_2.[31] Reproduced with permission from reference 31. Copyright ACS (2012).

3. Molecular engineering of dyes to inhibit or suppress dye aggregation in DSSCs

Dye aggregation in DSSCs is most commonly regarded as a phenomenon that is best to be avoided. Fortunately, several ways have been established that can inhibit or suppress the formation of dye aggregates. These can be classified into three options: altering the innate chemistry of the dye molecule; altering the dye sensitization conditions during the DSSC fabrication process; or altering the environment of the dye···TiO_2 interface.

3.1 Obviating dye aggregation by altering the innate chemistry of the dye molecule

3.1.1. Molecular planarity of the dye

Planar molecules are especially prone to H-aggregation, which is generally undesirable for DSSC applications (*vide supra*). In order to diminish the extent of molecular planarity, aggregation-free organic dyes with a twisted π-conjugation (**32**) have been developed by Numata *et al*.[77] Compared with the corresponding planar dye (**33**), the twisted dye does not form aggregates, and the addition of co-adsorbing agents to **33** has a negligible influence on its absorption spectrum.

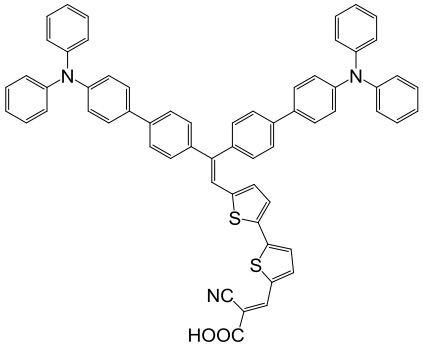

32

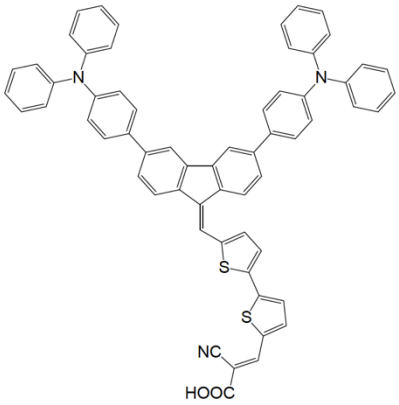

33

Two mono-anchor dye molecules of **34** were synthetically bridged to form a di-anchor dye (**35**), which exhibits a non-planar conformation. This bridging feature impedes aggregation of the dye when adsorbed onto TiO_2, yielding an enhanced PCE.[78] Additional side groups, such as pentafluorophenyl or cyanophenyl substituents, can be linked to the molecular backbone of a similar type of DSSC dye to form aggregation-free dyes **36** and **37**. Aggregation is circumvented via the rotation of the additional substituent about the *ipso* carbon atom that is attached to the nitrogen atom of the pyrrole group. These

organic dyes exhibit PCEs that are close to that of the DSSC benchmark N719 (**38**).[79] Nonplanar triphenylamine groups and nonplanar butterfly-shaped molecular building blocks based on phenothiazine also inhibit molecular aggregation of the dyes.[72,77,80]

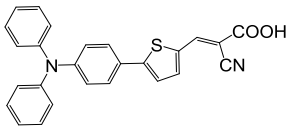

34

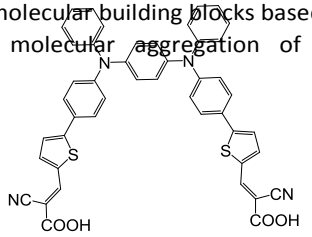

35

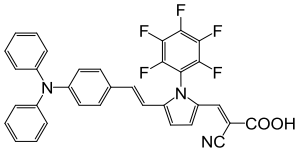

36

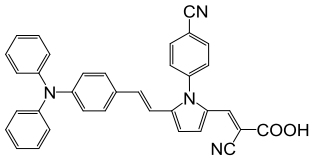

37

3.1.2. Adding alkyl groups and bulky substituents to the dye

Introducing long-chain alkyl groups is another commonly employed method to impede dye aggregation in DSSCs.[81] The length of the alkyl chain is important for tuning the optoelectronic properties of the DSSC. The introduction of long alkyl chains to a dye results in slower charge-recombination dynamics to both the dye cation and the redox electrolyte; see, for example, **17** and **39**.[82] Tuning bulky methoxy chains led to the enhancement of PCE in a series of organic D-π-A dyes with thienothiophene and cyanoacrylic acids (**40**,**41**), whereby **41** contains the longest chain (hexyloxy) of these two dyes and correspondingly exhibits the highest PCE.[83] Hydrophobic hexyloxy groups have been attached to the donor group of the triphenylamine-based dyes **41** and **42** in order to reduce aggregation, which resulted in an overall PCE of over 7%.[84] An alkylphenyl chain has been introduced in the ladder-type pentaphenylene dye **43** to disturb the π···π stacking.[85] For a series of benzothiazole merocyanine dyes, the aggregation behavior has been examined as a function of the alkyl chain length: dyes with longer alkyl chains exhibited J-aggregation on TiO_2, increased PCE values, and enhanced photostability relative to dyes with shorter alkyl chains.[74] It has accordingly been proposed that the alkyl-chain-induced formation of J-aggregates may prevent isomerization by restricting internal rotation, which should improve the stability of the DSSCs.[74] Side groups based on aromatic rings and methyl groups that have been introduced in e.g. diphenyldibenzofulvene-based sensitizers, led to a diminution of intermolecular interactions and J-type arrangements of the dyes on the TiO_2 surface.[86]

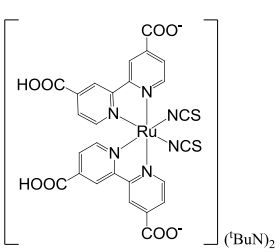

38

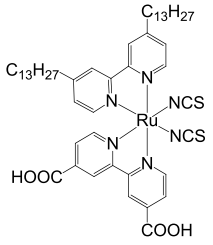

39

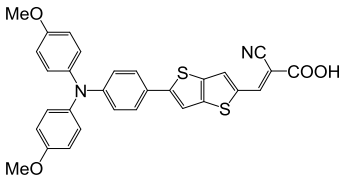

40

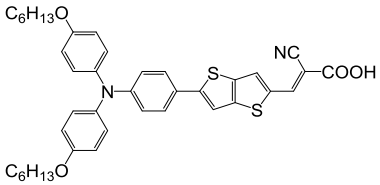

41

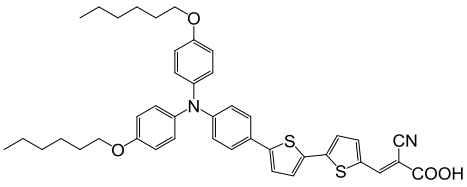

42

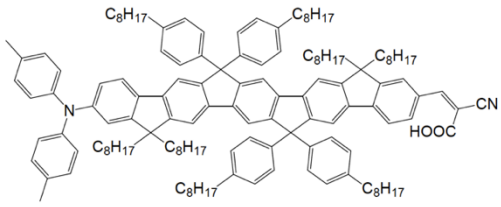

43

3.1.3. Changing the chemical nature or substitution position of the anchoring group on the dye

Aggregation may also be affected by changing the nature of the anchoring group on a dye. For example, the angle that a dye molecule subtends to the TiO_2 surface upon adsorption can be altered by changing the position of the dye anchoring group. Such an alteration has afforded control over the tendency for dye aggregation in zinc phthalocyanine (**44**)-sensitized solar cells;[87] the judiciously substituted dye **44** is void of any significant effects of dye aggregation. The combination of catechol axial attachment and *tert*-butyl peripheral groups in **45** allows efficient sensitization in the absence of co-adsorbents and dye aggregation.[88] The relative positions of the xanthylium core and the surface-binding anchoring groups determine whether dye **23** (where E = O) forms H-aggregates.[89] Selenorhodamine dyes with carboxylic (**46**), hydroxamic (**47**), or phosphonic acid (**48**) anchoring groups exhibit different aggregation modes, which is reflected in different absorption bands in their UV/vis absorption spectra.[90] Considering the chemical nature of anchoring groups, first-principles

This journal is © The Royal Society of Chemistry 20xx

calculations and molecular dynamics (MD) simulations have predicted that dyes with -CSSH anchoring groups (**49**) are less prone to dye aggregation due to weaker intermolecular hydrogen bonding.[91]

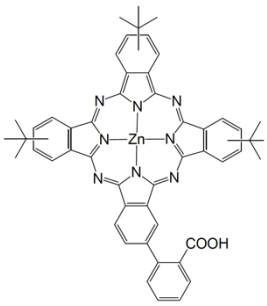

44

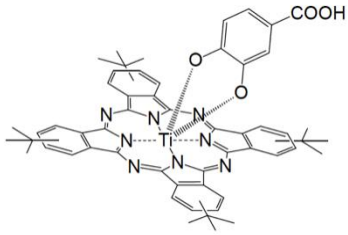

45

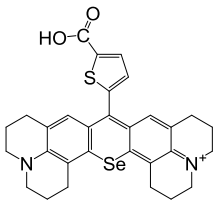

46

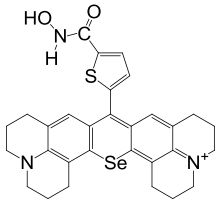

47

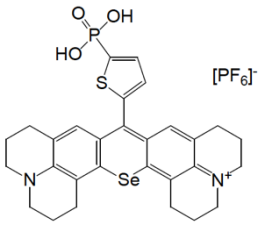

48

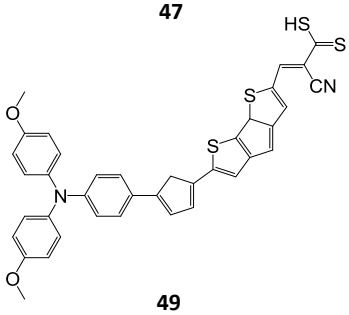

49

3.2 Obviating dye aggregation by altering the dye sensitization conditions during the DSSC fabrication process

3.2.1 Adding co-adsorbing agents to the dye solution

The sole function of a co-adsorbing agent is to suppress undesirable dye aggregation by adding it to the dye solution during the sensitization of the DSSC. When electrodes with sintered TiO_2 films are exposed to solution(s) containing dye(s) and co-adsorbing agent(s), both adsorbents compete for anchoring spaces on the TiO_2 surface. Cholic acid (CA, **50**) and chenodeoxycholic acid (CDCA, **51**) (Figure 10), as well as their derivatives, are frequently used as co-adsorbing agents.[92–94] The co-adsorbing agents usually contain a carboxylic acid anchoring group and an alkyl chain with aromatic groups to suppress intermolecular coupling.

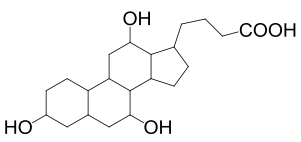

50

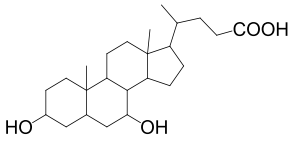

51

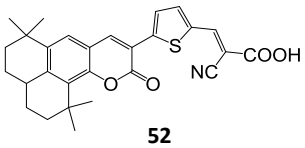

52

Hara *et al.* have studied the interaction between CDCA and coumarin dye **52**, which is prone to aggregation upon adsorption onto TiO_2, where the dye is sensitized alone.[95,121] The modelled structure revealed a distance of ~3 Å between the molecules of CDCA and those of coumarin on the surface of a $(TiO_2)_{82}$ substrate. An increased interaction energy was found which denoted the replacement of dye···dye dimers with CDCA···dye dimers (Figure 9), suggesting a favorable co-adsorption of CDCA and dye molecules, and an effective suppression of homodimer dye···dye stacking.[95,121]

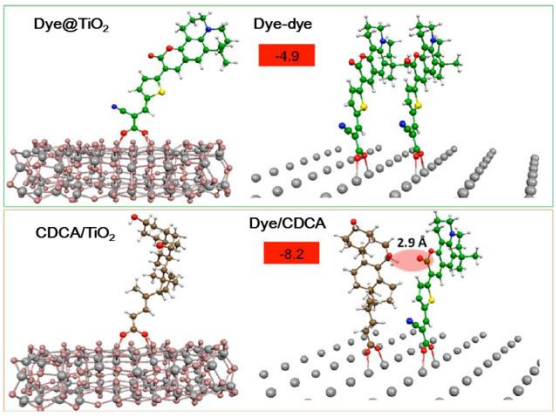

Figure 9 Left: optimized ground-state geometries for **52** (top panel) and CDCA on the surface of a $(TiO_2)_{82}$ substrate (bottom panel). Right: close interactions between **52**···**52** homodimer (top panel) and a CDCA···**52** heterodimer (bottom panel), together with the corresponding interaction energies, -4.9 and -8.2 kcal/mol, respectively.[95] Reproduced with permission from reference 95. Copyright ACS (2013).

The effect of adding CDCA to a DSSC based on indoline dye D149 (**53**), which was electrodeposited on porous ZnO, has been studied in detail.[96] To achieve high PCEs, control over the adsorption time and use of co-adsorbing agents were essential. Using higher concentrations of CDCA led to longer lifetimes of the excited dyes on the ZnO substrate due to the suppression of aggregation–induced quenching.[96]

CDCA has also been co-adsorbed with Zn-porphyrin dyes **54**, **55** and **56**, and the addition of CDCA improved the PCEs of all sensitizers except for **55** with long alkyl groups.[97] The carbazole-substituted triphenylamine-based organic dye **57** deposited on alumina and TiO_2 nanoparticles showed blue-shifted emission bands and longer excited-state lifetimes in the presence of CDCA; effects that were attributed to reduced dye aggregation.[98] For TiO_2 electrodes sensitized with Zn-phthalocyanine dye **58**, the quantity of co-adsorbent allows control over the degree of aggregation, while femtosecond transient absorption measurements revealed that the injection

yield of phthalocyanine **59** was essentially void of aggregation-induced recombination.[87]

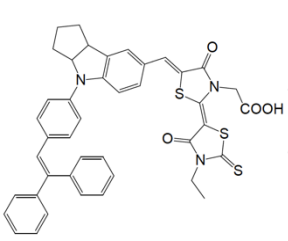

53

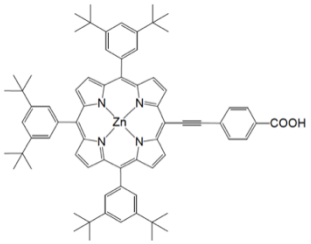

54

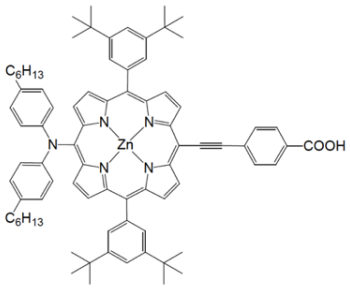

55

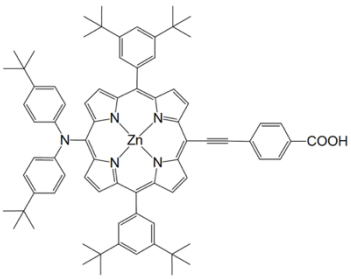

56

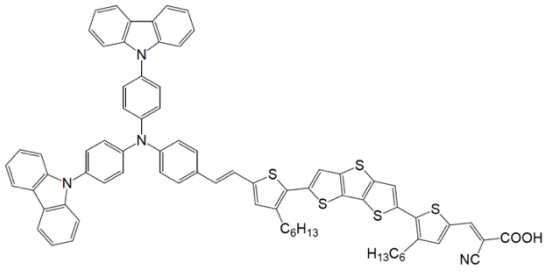

57

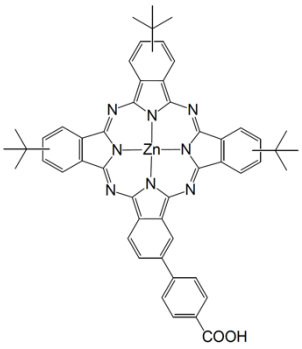

5

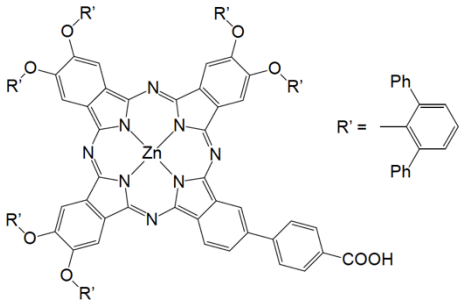

59

CDCA derivatives suppress aggregation of the Black Dye (**16**) during the sensitization of TiO_2 films by forming stronger hydrogen bonds with the dye molecules.[99, 100]

For squaraine dye **60**, the presence of the co-adsorbent CDCA avoids the formation of H-aggregates, and leads to the detection of two transient species corresponding to a monomer and a radical cation.[102] Morandeira *et al.* studied the effects of the presence of CDCA on the non-aggregated dye **61** and found that even though the injection kinetics and yield are not affected by the addition of co-adsorbents, the electron recombination with the dye cations was retarded.[103] This result possibly owes itself to the fact that the co-adsorbent increases the tilt angle of the adsorbed dyes, affecting the distance between the TiO_2 surface and the dye orbitals.

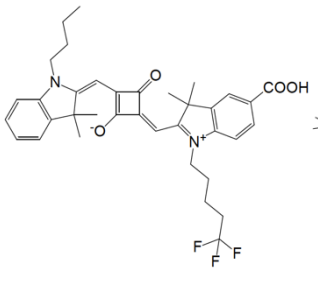

60

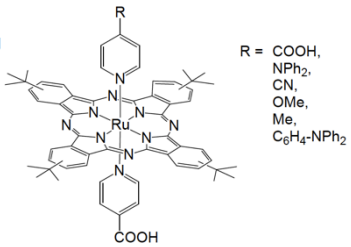

61

3.2.2 Changing the solution conditions of dye sensitization

This journal is © The Royal Society of Chemistry 20xx

Varying parameters that are associated with the solution conditions of the dye sensitization process will often influence the ability of the dye aggregates to form.[105] These conditions include: the dye concentration in the sensitizing solution; the solvent choice for this solution; and the sensitization time by which the dye is exposed to the TiO_2 surface. For example, in the case of the Ru-based dye N3 (**62**), long sensitization times promote dye aggregation, as the dye loading increases with exposure time, resulting in a decreased PCE.[106] Nevertheless, for other dyes, such as **63**, adsorption saturation of TiO_2 films in dye solution occurs only after several hours, which suggests the spontaneous formation of a monolayer.[106]

Several examples nicely illustrate how the sensitization solvent can significantly influence the formation of aggregates. For the anionic merocyanine dye **64**, sensitization in acetonitrile leads to the simultaneous formation of aggregates and monomers on nanostructured TiO_2 films,[107] while sensitization in Aerosol-OT/heptane solutions leads to the predominant formation of monomers. The IPCE of the monomer is nearly five times higher than that of the aggregates, while a significantly higher fluorescence quantum yield and excited singlet lifetime can be observed for dyes dissolved in heptane rather than in acetonitrile.[107]

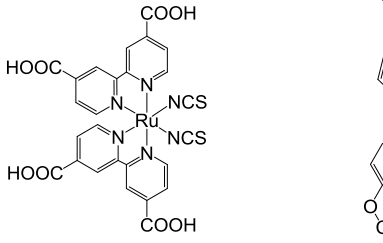

62

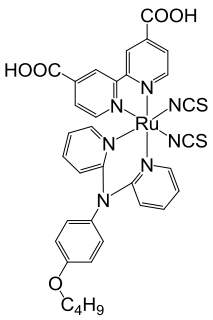

63

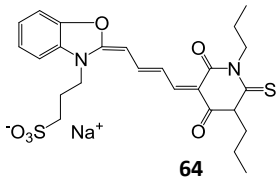

64

3.2.3 Employing host-guest media

Host-guest systems in solution represent an effective method to manipulate the formation of H- and J-aggregates and thus control dye aggregation. For example, the host cucurbit[7]uril disrupts the formation of J-aggregates of the pseudoisocyanine dye **65** and the formation of H-aggregates of the pseudoisocyanol dye **66**, taking advantage of the binding properties of the cucurbit[7]uril host.[108,109] Introducing anionic polyelectrolytes in the presence of a host enhances the formation of cationic cyanine dye aggregates in aqueous media.[109] However, such host-guest systems have not yet been directly applied to suppress unwanted dye aggregation in DSSCs. One highly interesting application would be the use of host-guest systems to control dye aggregation in the solid form on TiO_2 substrate.

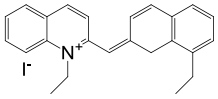

65

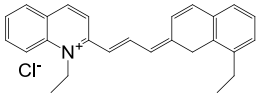

66

3.2.4 Dye co-sensitization

Dye co-sensitization is the process by which two or more chemically different dyes are sensitized onto the surface of a TiO_2 thin film to form a DSSC working electrode. At first sight, a dye co-sensitizer may seem somewhat like a co-adsorbing agent that was described in section 3.2.1. However, while a dye co-sensitizer may inhibit or help suppress dye aggregation, as is the function of a co-adsorbing agent, the primary purpose of a dye co-sensitizer is to add functionality to the DSSC in its own right as a dye. For example, the use of two chemically different dyes in a DSSC, whose UV/vis absorption wavelengths are complementary, can result in panchromatic absorption; thus, the DSSC device presents greater light-harvesting efficiency.[6,68,110–112] If dye co-sensitization can thus reduce dye aggregation as well, this offers a 'win-win' situation for DSSC device technology. A stepwise molecular engineering approach has been adopted to design a panchromatic response in co-sensitized DSSCs,[113] whereby fluorescein dye derivatives exhibiting extended optical absorption up to 500 nm have been shown to be suitable co-sensitizers for DSSC applications.[114] Meanwhile, when co-sensitized with the Ru-based dye **67**, the phthalocyanine dye **68**, which is incapable of hole regeneration, can produce a photocurrent via intermolecular energy transfer with an average excitation-transfer efficiency of > 25%, boosting light harvesting from 700 to 800 nm.[115]

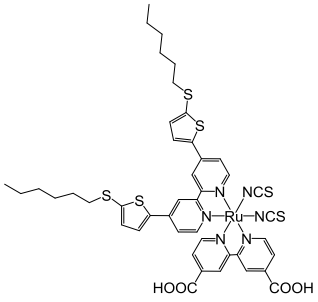

67

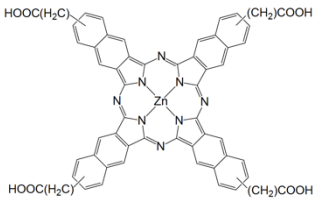

68

When co-sensitized with the energy-relay dye (ERD) **69**, which is a highly photoluminescent chromophore, **70** on TiO_2 undergoes Förster resonance energy transfer (FRET), which allows a broader spectral absorption, an increase in dye loading, and an enhanced PCE. A typical absorption process in DSSCs with FRET is characterized by: i) light absorption by the sensitizing dye, ii) initial absorption of higher-energy photons by the ERD, iii) FRET from the ERD to the sensitizing dye (Figure 10).[116] A 35% improvement in the photovoltaic performance of zinc phthalocyanine dye **70** was observed due to FRET when it was co-sensitized with the two ERDs **71** and **72**.[117] The FRET method has also been investigated in standard DSSCs sensitized

Please do not adjust margins

with Ru-based dye N719 (**38**), which led to an improvement of the optoelectronic properties of the device.[118]

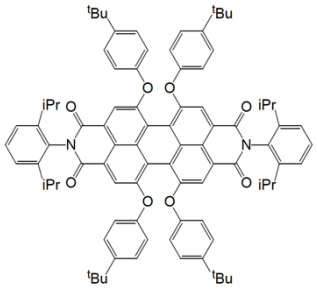

69

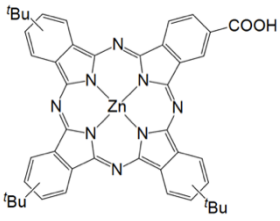

70

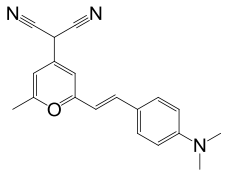

71

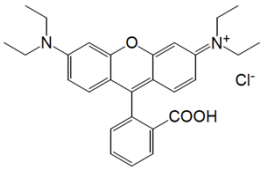

72

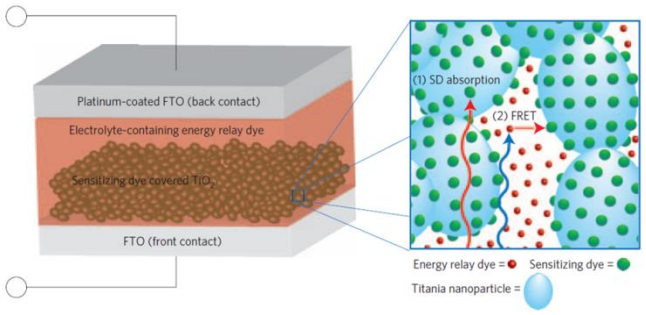

Figure 10 Schematic representation of a DSSC containing energy-relay dyes for FRET.[116] Reproduced with permission from reference 116. Copyright Macmillan Publishers Limited (2009).

Co-sensitizers based on donor–acceptor-type molecules have also shown that they can provide added value to their intrinsic use as a complementary light harvester. For example, dyes **73** and **74**, which exhibit intense absorption at 350-400 nm, have been added to DSSCs sensitized with the Black Dye (**16**), to afford an increase in the PCE of the solar cell from 10.7% to 11.4%.[101] This improvement in device performance arises because the addition of these donor–acceptor type molecules also adjusts the separation between molecules of **16** to avoid aggregation, counterbalances the competitive absorption of visible light by the electrolyte (I^-/I_3^-), and reduces the extent of electron recombination in the TiO_2 film.[101] In another example, chemisorption of the porphyrin **75** in the presence of fullerene molecules, functionalized with carboxylic acid anchors on the surface of semiconductor substrates, resulted in reduced aggregation.[104]

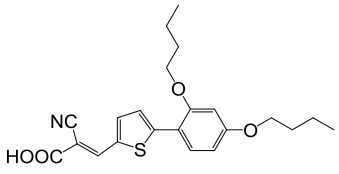

73

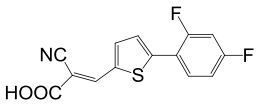

74

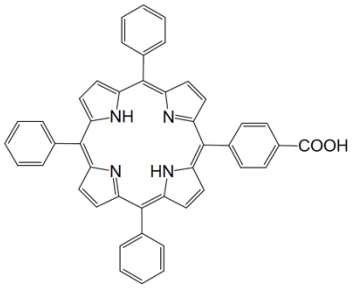

75

3.3. Obviating dye aggregation by altering the environment of the dye···TiO_2 interface

3.3.1 Atomic layer deposition (ALD)

As dye aggregation often quenches the excited states of the dyes and limits the yield of electron injection into the semiconductor substrate, surface treatment strategies, such as atomic layer deposition (ALD) have been employed to minimize dye interactions caused by aggregation and the associated ultrafast dye aggregate excited-state relaxation processes. ALD effectively fills the gaps between adsorbed dye molecules with ultrathin layers of either TiO_2 or Al_2O_3, thereby preventing aggregation (Figure 11). Prior to ALD, intermolecular interactions are usually severe, while dye interactions are retarded due to the isolation of the dyes after ALD. Following ALD, the rate of electron recombination from the injected electrons in TiO_2 to the oxidized form of the redox shuttle is attenuated.[119] In the case of solar cells employing an archetypal donor–acceptor organic dye such as **76**, ALD is more effective than co-adsorbing agents, and the ALD post-treatment induces an increase of more than 30% in overall PCE of the solar cell, while it does not interfere with dye/semiconductor electronic coupling.[119] Apart from aggregation, ALD also prevents desorption of dyes from the photoelectrode, which is one of the major limitations for the longevity of DSSCs.[120]

This journal is © The Royal Society of Chemistry 20xx

Please do not adjust margins

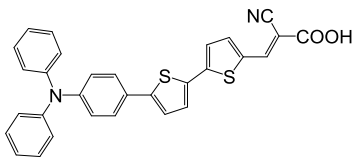

76

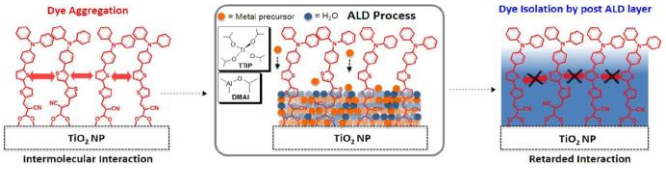

Figure 11 Schematic diagram for post-sensitization ALD on TiO_2 nanoparticles. The gaps between adsorbed dye molecules on standard nanoparticles can be efficiently filled with ultrathin layers of either TiO_2 or Al_2O_3.[119] Reproduced with permission from reference 119. Copyright ACS (2015).

3.3.2 Electrolyte additives

In the presence of Li^+ cations, 4-tert-butylpyridine (TBP, **77**) adsorbs on dye-sensitized TiO_2 films, and suppresses the dark current on the TiO_2 surface, which improves the photovoltage of the solar cell in a manner similar to CDCA.[121] Substituted benzene derivatives such as bromobenzene (**78**), anisole (**79**), benzene (**80**), and iodobenzene (**81**) have been included in DSSC electrolytes to penetrate dye layers and form stable complexes, which can lead to an increased quenching of excited states and enhanced charge-separation efficiency of the DSSC. Similar to the ALD method, electrolyte additives inhibit the recombination between electrons in the semiconductor and the oxidized electrolyte, thus increasing V_{oc}.[122]

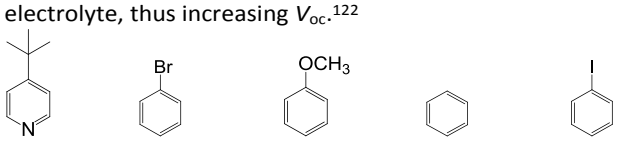

77 **78** **79** **80** **81**

4. Aggregation in related optoelectronic phenomena

In this review, we have discussed the impact of dye aggregation on the performance of DSSCs. In fact, dye aggregation not only strongly influences DSSC performance, but also affects several optoelectronic parameters and devices. Molecular aggregation is common in a variety of optoelectronic systems, including dye-sensitized water-splitting systems, molecularly-modified solar cells, aggregation-induced emission (AIE) systems, nonlinear optics, and organic transistors.[123]

The photoanode of dye-sensitized water-splitting systems is very similar to that of DSSCs, both of which use a dye to absorb light and convert it into an electrical current. In the dye-sensitized water-splitting photoanode, molecular aggregation can be controlled by molecular co-adsorption and the ALD method.[124]

In organic solar cells, light absorption is critical and it can be controlled by molecular aggregation. For example, H- and J-aggregates can be formed selectively via a judicious choice of solvents, resulting in a difference in photovoltaic performance of organic solar cells based on squaraine/fullerene bilayer heterojunction photovoltaic cells.[125] Molecular aggregation on the surface of CdTe solar cells has been employed to produce AIE, and thus convert unfavorable photons in the UV region into favorable photons in the NIR region.[126]

Dye aggregation has also been investigated extensively to control emission phenomena.[127,128] Dye aggregation on nanoparticles has found applications in bioimaging, where one- and two-photon fluorescence is enhanced via manipulation of dye aggregation to minimize intermolecular quenching, which enables a remarkable improvement of signals in bioimaging.[129] A host-guest complex serves as a template for the formation of H-aggregates of thiazole orange molecules, which does not exhibit fluorescence in aqueous solutions, and presents a well-resolved fluorescence spectrum.[130] Molecular engineering methods, such as introducing bulky peripheral groups, have been employed to enhance fluorescence by hindering aggregation via steric congestion.[131]

In nonlinear optics (NLO), light absorption is critical for achieving frequency modulation. J-aggregation induces a doubling of the second-order NLO response, which is associated with a narrow and intense band in the absorption spectrum that is red-shifted relative to that of the isolated NLO material.[132,133] J-aggregation has been applied in organic transistors in order to induce lower carrier mobilities of electrons and holes with respect to the mobilities of the H-aggregation mode.[134] Conversely, the large π-overlap in materials based on H-aggregates facilitates significantly higher carrier mobilities due to the inherently higher levels of packing order and the stable morphologies, which leads to a highly reproducible performance.[135]

5. Other materials characterization methods to probe dye aggregation

A key barrier to a better understanding of dye aggregation is the lack of structural information about this phenomenon at the molecular scale. One way to overcome this barrier is to use a greater variety of materials characterization methods to understand dye aggregation. This review has necessarily focused on results from UV/vis spectroscopy, since this acts by far as the primary tool to understand dye aggregation at the molecular scale. However, there are a few examples of studies that demonstrate the application of other materials characterization methods to the study of dye aggregation on DSSCs.

Other optical probes such as emission spectroscopy, time-resolved emission spectroscopy, and transient absorption spectroscopy have been used to determine lifetimes and decay channels of electronic states that comprise the exciton bands

Please do not adjust margins

created by dye aggregation.[31] Photoelectron spectroscopy has been used to infer surface effects of aggregation of dyes on a ZnO semiconductor surface,[136] while bulk effects on the same were observed indirectly from complementary infra-red and Raman spectroscopy and electrochemical studies.[137] Photoelectrochemical techniques such as *I-V* curves, incident-photon-to-current efficiency (IPCE) measurements, and impedance spectroscopy can also be used to evidence indirect manifestations of dye aggregation.[138,139]

More direct structural information about dye aggregation can be obtained at the molecular scale, via atomic imaging and scattering techniques. For example, atomic force microscopy has demonstrated that dyes can stack on top of each other to form multilayers of dye aggregates on TiO_2 surfaces,[58,140] and that dye coverage can be inhomogeneous,[140] *i.e.*, not necessarily occur in the homogeneous distribution of dye monolayers on TiO_2 surfaces that has historically been assumed. Scanning tunneling microscopy (STM) has produced similar findings.[57] Meanwhile, combining STM with scanning tunneling spectroscopy (STS) capabilities has revealed the first direct evidence for dye molecules adsorbing onto TiO_2 with multi-conformational variation, including a dimer as one such variant.[141] This STM/STS study has challenged the historical view that dyes anchor onto TiO_2 in only one structural form and that molecular aggregates of dyes need to be considered as one possible form. Such structural variations not only affect the spatial considerations of dyes on the TiO_2 surface, but also the the energetics of the DSSC working electrode: multiple structural forms of dyes yield multiple LUMO energies that, in turn, produce multiple driving forces for electron injection in the DSSC device.

The propensity for dye aggregation and likely structural types can be anticipated from X-ray crystallography,[142-145] whose three-dimensional structural determination of dye molecules can also support[142,143] X-ray reflectometry (XRR) studies. To this end, XRR has demonstrated its use in quantifying the average molecular orientation of dyes on TiO_2 surfaces[5,146,147] and inferring the nature of dye···dye intermolecular interactions therein;[5,147] such interactions may describe dye aggregation in either the lateral or longitudinal projection to the TiO_2 surface. These are *ex situ* XRR studies in the sense that they provide information on the dye···TiO_2 interfacial structure of the exposed DSSC working electrode, while this electrode becomes a buried interface once embedded within its device environment. A recent *in situ* neutron reflectometry (NR) study[147] has demonstrated that the same type of structural information discerned from XRR can be determined, but on the dye···TiO_2 interface as it manifests within a DSSC device environment. The NR study revealed that the structure of this buried interface was altered by the presence of the electrolyte in the device. This highlights the importance of such *in situ* structural studies and opens a new path for exploring the nature of dye aggregation within a DSSC device medium.

6. Conclusions

Recent experimental and theoretical studies on dye aggregation in DSSCs have revealed aggregate structures at the nanoscale. Their influence on photovoltaic properties has promoted the development of improved methods to understand and thence control dye aggregation on semiconductor substrates to fit specific device requirements. The optical properties of dye aggregates can be described by Kasha's molecular exciton theory.[15] The excitation energy of a dye dimer depends on the arrangement of the molecular dipole moments. Face-to-face alignment of molecules, and therefore molecular dipoles, yields H-aggregates, which are associated with hypsochromic shifts of the light-absorption spectra; conversely, J-aggregates are obtained for edge-to-edge arrangements of the dipole moments. Whether a specific dye forms H- or J-aggregates strongly depends on the molecular structure of the dye, and parameters of the deposition process. Unfortunately, a universal law to reliably predict the formation of H- or J-aggregates for a given dye does not yet exist. However, dye aggregation can be manipulated to some extent via molecular engineering methods. These may involve a chemical means to reduce molecular planarity of a dye, by adding bulky, hydrophobic, or other substituents, or vary the nature and position of the dye anchoring group. Alternatively, the dye-sensitization conditions may be modified via atomic layer deposition, or the use of electrolyte additives or co-adsorption agents. The judicious selection of dye-sensitization time, concentration, and the type of solvent will also impact the nature of the dye···TiO_2 interface that comprises the working electrode.

Certain types of dye aggregates can even improve the performance of DSSCs, and also those of other optoelectronic devices that rely on dye molecules, such as water-splitting systems, organic solar cells, light-emitting systems, and non-linear optical devices. While it is not currently possible to determine *a priori* if dye aggregation augments or depletes the desired photovoltaic or optoelectronic effect, a better understanding of dye aggregates at the molecular level will inevitably lead to device improvements in a variety of DSSC and optoelectronic media. To this end, increasing the prevalence of studies on dye aggregation that engage a much wider remit of materials characterization methods will undoubtedly help in realizing better options for the molecular engineering of DSSC dyes and related optoelectronic phenomena.

Conflicts of Interest

There are no conflicts of interest to declare.

Acknowledgements

J.M.C. would like to thank the 1851 Royal Commission for the 2014 Design Fellowship hosted by Argonne National Laboratory, where work done was supported by DOE Office of Science, Office of Basic Energy Sciences, under contract No. DE-AC02-06CH11357. L.Z. acknowledges support by Nanjing University of

 This journal is © The Royal Society of Chemistry 20xx

Please do not adjust margins

Please do not adjust margins

Information Science and Technology (NUIST) Startup Fund, the Jiangsu Provincial Natural Science Foundation (Grant BK20160942), Jiangsu Province "Double Plan" (Grant 2191131700501/R2016SCB02), the National Natural Science Foundation of China (Grant No. 51702165), the Nanjing Technology Foundation for Selected Overseas Chinese Scholar, Ministry of Personnel of China (Grant 2191011606901/R2016LZ01) and the Natural Science Fund for Colleges and Universities in Jiangsu Province (Grant 16KJB150027).

References

1 M. Grätzel, *Nature*, 2001, **414**, 338–44.
2 B. O'Regan and M. Grätzel, *Nature*, 1991, **353**, 737–740.
3 M. Grätzel, *J. Photochem. Photobiol. C Photochem. Rev.*, 2003, **4**, 145–153.
4 M. K. Nazeeruddin, P. Péchy, T. Renouard, S. M. Zakeeruddin, R. Humphry-Baker, P. Comte, P. Liska, L. Cevey, E. Costa, V. Shklover, L. Spiccia, G. B. Deacon, C. a Bignozzi and M. Grätzel, *J. Am. Chem. Soc.*, 2001, **123**, 1613–1624.
5 J. McCree-Grey, J. M. Cole and P. J. Evans, *ACS Appl. Mater. Interfaces*, 2015, **7**, 16404–16409.
6 N. Robertson, *Angew. Chem. Int. Ed.*, 2006, **45**, 2338–2345.
7 L. Zhang, X. Liu, W. Rao and J. Li, *Sci. Rep.*, 2016, **6**, 35893.
8 L. Zhang and J. M. Cole, *ACS Appl. Mater. Interfaces*, 2014, **6**, 15760–15766.
9 T. Marinado, K. Nonomura, J. Nissfolk, M. K. Karlsson, D. P. Hagberg, L. Sun, S. Mori and A. Hagfeldt, *Langmuir*, 2010, **26**, 2592–2598.
10 F. Labat, T. Le Bahers, I. Ciofini and C. Adamo, *Acc. Chem. Res.*, 2012, **45**, 1268–1277.
11 T. W. Hamann, R. A. Jensen, A. B. F. Martinson, H. Van Ryswyk and J. T. Hupp, *Energy Environ. Sci.*, 2008, **1**, 66.
12 A. Hagfeldt, G. Boschloo, L. Sun, L. Kloo and H. Pettersson, *Chem. Rev.*, 2010, **110**, 6595–6663.
13 L. Zhang and J. M. Cole, *ACS Appl. Mater. Interfaces*, 2015, **7**, 3427–3455.
14 C. J. Bardeen, *Annu. Rev. Phys. Chem.*, 2014, **65**, 127–148.
15 M. Kasha, H. R. Rawls and M. A. El-Bayoumi, *Pure Appl. Chem.*, 1965, **11**, 371–392.
16 T. Etienne, L. Chbibi, C. Michaux, E. A. Perpète, X. Assfeld and A. Monari, *Dyes Pigm.*, 2014, **101**, 203–211.
17 V. Czikklely, H. D. Forsterling and H. Kuhn, *Chem. Phys. Lett.*, 1970, **6**, 207–210.
18 M. Sauer, J. Hofkens and J. Enderlein, *Handbook of Fluorescence Spectroscopy and Imaging*, Wiley-VCH, Weinheim, Germany, 2011.
19 T. Biver, A. Boggioni, F. Secco, E. Turriani, M. Venturini and S. Yarmoluk, *Arch. Biochem. Biophys.*, 2007, **465**, 90–100.
20 W. G. Herkstroeter and S. Farid, *J. Am. Chem. Soc.*, 1990, 3583–3589.
21 A. R. Monahan and D. F. Blossey, *J. Phys. Chem.*, 1970, **74**, 4014–4021.
22 K. Hamada, T. Iijima and S. Amiya, *J. Phys. Chem.*, 1990, **94**, 3766–3769.
23 R. S. Stoll, N. Severin, J. P. Rabe and S. Hecht, *Adv. Mater.*, 2006, **18**, 1271–1275.
24 F. Nüesch and M. Grätzel, *Chem. Phys.*, 1995, **193**, 1–17.
25 M. H. Habibi, A. Hassanzadeh and A. Zeini-Isfahani, *Dyes Pigm.*, 2006, **69**, 111–117.
26 P. Kubát, K. Lang, P. Janda and P. Anzenbacher, *Langmuir*, 2005, **21**, 9714–9720.
27 G. Pescitelli, L. Di Bari and N. Berova, *Chem. Soc. Rev.*, 2014, **43**, 5211-5233.
28 J. A. Gutierrez, R. D. Falcone, J. J. Silber and N. M. Correa, *J. Phys. Chem. A*, 2010, **114**, 7326–7330.
29 T. D. Slavnova, H. Görner and A. K. Chibisov, *J. Phys. Chem. B*, 2011, **115**, 3379–3384.
30 J. Guasch, L. Grisanti, M. Souto, V. Lloveras, J. Vidal-Gancedo, I. Ratera, A. Painelli, C. Rovira and J. Veciana, *J. Am. Chem. Soc.*, 2013, **135**, 6958–6967.
31 S. Verma and H. N. Ghosh, *J. Phys. Chem. Lett.*, 2012, **3**, 1877–1884.
32 T. Chemistry, *Jsdc*, 1993, **109**, 120–122.
33 K. K. Karukstis, L. A. Perelman and W. K. Wong, *Langmuir*, 2002, **18**, 10363–10371.
34 K. Rohatgi and G. Singhal, *J. Phys. Chem.*, 1966, **70**, 1695–1701.
35 S. Yefimova, A. Lebed, A. Sorokin, G. Guralchuk, I. Borovoy and Y. Malyukin, *J. Mol. Liq.*, 2012, **165**, 113–118.
36 P. Skrabal, F. Bangerter, K. Hamada and T. Iijima, *Dyes Pigm.*, 1987, **8**, 371–374.
37 A. Navarro and F. Sanz, *Dyes Pigm.*, 1999, **40**, 131–139.
38 M. Ferus-comelo and A. J. Greaves, *Color. Technol.*, 2002, **118**, 15–19.
39 D. C. Valdes-Aguiler, O., & Neckers, *Accounts Chem. Res.*, 1989, **22**, 171–177.
40 C. Ouyang, S. Chen, B. Che and G. Xue, *Colloids Surfaces A Physicochem. Eng. Asp.*, 2007, 301, 346–351.
41 R. F. Pasternack, C. Fleming, S. Herring, P. J. Collings, J. dePaula, G. DeCastro and E. J. Gibbs, *Biophys. J.*, 2000, **79**, 550–60.
42 D. D. Pant, C. L. Bhagchandani, K. C. Pant and S. P. Verma, *Chem. Phys. Lett.*, 1971, **9**, 546–547.
43 G. M. Walker and L. R. Weatherley, *Chem. Eng. J.*, 2001, **83**, 201–206.
44 R. B. McKay, *Trans. Faraday Soc.*, 1965, **61**, 1787–1799.
45 N. Kato, J. Prime, K. Katagiri and F. Caruso, *Langmuir*, 2004, **20**, 5718–5723.
46 X. Liu, J. M. Cole and K. S. Low, *J. Phys. Chem. C*, 2013, **117**, 14723–14730.
47 C. Peyratout and L. Daehne, *Phys. Chem. Chem. Phys.*, 2002, **4**, 3032–3039.
48 L. Zhang, J. M. Cole and X. Liu, *J. Phys. Chem. C*, 2013, **117**, 26316–26323.
49 T. D. Slavnova, A. K. Chibisov and H. Görner, *J. Phys. Chem. A*, 2002, **106**, 10985–10990.
50 A. K. Chibisov and H. Görner, *Chem. Phys. Lett.*, 2002, **357**, 434–439.
51 T. D. Slavnova, A. K. Chibisov and H. Görner, *J. Phys. Chem. A*, 2005, **109**, 4758–4765.

Please do not adjust margins

Please do not adjust margins

52 H. Ozawa, M. Awa, T. Ono and H. Arakawa, *Chem. Asian J.*, 2012, **7**, 156–162.

53 G. Marotta, M. A. Reddy, S. P. Singh, A. Islam, L. Han, F. De Angelis, M. Pastore and M. Chandrasekharam, *ACS Appl. Mater. Interfaces*, 2013, **5**, 9635–9647.

54 S. Feng, Q.-S. Li, P.-P. Sun, T. A. Niehaus and Z.-S. Li, *ACS Appl. Mater. Interfaces*, 2015, **7**, 22504–22514.

55 S. Feng, Q. S. Li, T. A. Niehaus and Z. S. Li, *Org. Electron. physics, Mater. Appl.*, 2017, **42**, 234–243.

56 S. Feng, Q.-S. Li, L.-N. Yang, Z.-Z. Sun, T. A. Niehaus and Z.-S. Li, *J. Power Sources*, 2015, **273**, 282–289.

57 M. Ikeda, N. Koide, L. Han, A. Sasahara and H. Onishi, *Langmuir*, 2008, **24**, 8056–8060.

58 K. Y. Liu, C. L. Hsu, J. S. Ni, K. C. Ho and K. F. Lin, *J. Colloid Interface Sci.*, 2012, **372**, 73–79.

59 K. R. Mulhern, M. R. Detty and D. F. Watson, *J. Phys. Chem. C*, 2011, **115**, 6010–6018.

60 K. R. Mulhern, A. Orchard, D. F. Watson and M. R. Detty, *Langmuir*, 2012, **28**, 7071–7082.

61 S. Okada and H. Segawa, *J. Am. Chem. Soc.*, 2003, **125**, 2792–2796.

62 F. Würthner, T. E. Kaiser and C. R. Saha-Möller, *Angew. Chemie Int. Ed.*, 2011, **50**, 3376–3410.

63 A. Ehret, L. Stuhl and M. T. Spitler, *J. Phys. Chem. B*, 2001, **105**, 9960–9965.

64 X.-F. Wang, Y. Koyama, H. Nagae, Y. Yamano, M. Ito and Y. Wada, *Chem. Phys. Lett.*, 2006, **420**, 309–315.

65 X.-F. Wang, R. Fujii, S. Ito, Y. Koyama, Y. Yamano, M. Ito, T. Kitamura and S. Yanagida, *Chem. Phys. Lett.*, 2005, **416**, 1–6.

66 P. M. Sirimanne, *Renew. Energy*, 2008, **33**, 1424–1428.

67 N. Strataki, V. Bekiari, E. Stathatos and P. Lianos, *J. Photochem. Photobiol. A Chem.*, 2007, **191**, 13–18.

68 M. Ziółek, J. Karolczak, M. Zalas, Y. Hao, H. Tian and A. Douhal, *J. Phys. Chem. C*, 2014, **118**, 194–205.

69 L. Zhang and J. M. Cole, *ACS Appl. Mater. Interfaces*, 2014, **6**, 3742–3749.

70 L. Zhang, J. M. Cole and C. Dai, *ACS Appl. Mater. Interfaces*, 2014, **6**, 7535–7546.

71 L. Zhang and J. M. Cole, *Phys. Chem. Chem. Phys.*, 2016, **18**, 19062–19069.

72 L. Zhang, J. M. Cole, P. G. Waddell, K. S. Low and X. Liu, *ACS Sustain. Chem. Eng.*, 2013, **1**, 1440–1452.

73 Y. Hua, S. Chang, J. He, C. Zhang, J. Zhao, T. Chen, W.-Y. Wong, W.-K. Wong and X. Zhu, *Chem.-Eur. J.*, 2014, **20**, 6300–6308.

74 K. Sayama, S. Tsukagoshi, K. Hara, Y. Ohga, A. Shinpou, Y. Abe, S. Suga and H. Arakawa, *J. Phys. Chem. B*, 2002, **106**, 1363–1371.

75 Y. Amao and Y. Yamada, *Langmuir*, 2005, **21**, 3008–3012.

76 Y. Arai and H. Segawa, *Chem. Lett.*, 2013, **42**, 918–920.

77 Y. Numata, A. Islam, H. Chen and L. Han, *Energy Environ. Sci.*, 2012, **5**, 8548–8552.

78 R. Sirohi, D. H. Kim, S.-C. Yu and S. H. Lee, *Dyes Pigm.*, 2012, **92**, 1132–1137.

79 H. Li, L. Yang, R. Tang, Y. Hou, Y. Yang, H. Wang, H. Han, J. Qin, Q. Li and Z. Li, *Dyes Pigm.*, 2013, **99**, 863–870.

80 S. Agrawal, M. Pastore, G. Marotta, M. A. Reddy, M. Chandrasekharam and F. De Angelis, *J. Phys. Chem. C*, 2013, **117**, 9613–9622.

81 A. Otsuka, K. Funabiki, N. Sugiyama, H. Mase, T. Yoshida, H. Minoura and M. Matsui, *Chem. Lett.*, 2008, **37**, 176–177.

82 J. E. Kroeze, N. Hirata, S. Koops, M. K. Nazeeruddin, L. Schmidt-Mende, M. Grätzel and J. R. Durrant, *J. Am. Chem. Soc.*, 2006, **128**, 16376–16383.

83 M. F. Xu, R. Z. Li, N. Pootrakulchote, D. Shi, J. Guo, Z. H. Yi, S. M. Zakeeruddin, M. Grätzel, P. Wang and Y. Wang, *J. Phys. Chem. C*, 2008, **112**, 19770-19776.

84 J. H. Yum, D. P. Hagberg, S. J. Moon, K. M. Karlsson, T. Marinado, L. Sun, A. Hagfeldt, M. K. Nazeeruddin and M. Grätzel, *Angew. Chem. Int. Ed.*, 2009, **48**, 1576–1580.

85 G. Zhou, N. Pschirer, J. C. Schöneboom, F. Eickemeyer, M. Baumgarten and K. Müllen, *Chem. Mater.*, 2008, **20**, 1808–1815.

86 H. Li, R. Tang, Y. Hou, Y. Yang, J. Chen, L. Liu, H. Han, T. Peng, Q. Li and Z. Li, *Asian J. Org. Chem.*, 2014, **3**, 176–184.

87 H. Matsuzaki, T. N. Murakami, N. Masaki, A. Furube, M. Kimura and S. Mori, *J. Phys. Chem. C*, 2014, **118**, 17205–17212.

88 E. Palomares, M. V. Martínez-Díaz, S. A. Haque, T. Torres and J. R. Durrant, *Chem. Commun.*, 2004, 2112–2113.

89 J. R. Mann, M. K. Gannon, T. C. Fitzgibbons, M. R. Detty and D. F. Watson, *J. Phys. Chem. C*, 2008, **112**, 13057–13061.

90 M. W. Kryman, J. N. Nasca, D. F. Watson and M. R. Detty, *Langmuir*, 2016, **32**, 1521–1532.

91 S. Nachimuthu, W.-C. Chen, E. G. Leggesse and J.-C. Jiang, *Phys. Chem. Chem. Phys.*, 2016, **18**, 1071–1081.

92 T. Horiuchi, H. Miura, K. Sumioka and S. Uchida, *J. Am. Chem. Soc.*, 2004, **126**, 12218–12229.

93 K. Hara, T. Sato, R. Katoh, A. Furube, T. Yoshihara, M. Murai, M. Kurashige, S. Ito, A. Shinpo, S. Suga and H. Arakawa, *Adv. Funct. Mater.*, 2005, **15**, 246–252.

94 S. Ito, S. M. Zakeeruddin, R. Humphry-Baker, P. Liska, R. Charvet, P. Comte, M. K. Nazeeruddin, P. Péchy, M. Takata, H. Miura, S. Uchida and M. Grätzel, *Adv. Mater.*, 2006, **18**, 1202–1205.

95 Z.-S. Wang, Y. Cui, Y. Dan-oh, C. Kasada, A. Shinpo and K. Hara,. *J. Phys. Chem. C* 2011, **111**, 7224−7230.

96 A. El-Zohry, A. Orthaber and B. Zietz, *J. Phys. Chem. C*, 2012, **116**, 26144–26153.

97 H.-P. Lu, C.-Y. Tsai, W.-N. Yen, C.-P. Hsieh, C.-W. Lee, C.-Y. Yeh and E. W.-G. Diau, *J. Phys. Chem. C*, 2009, **113**, 20990–20997.

98 V. Dryza, J. L. Nguyen, T.-H. Kwon, W. W. H. Wong, A. B. Holmes and E. J. Bieske, *Phys. Chem. Chem. Phys.*, 2013, **15**, 20326-20332.

99 H. Kusama and K. Sayama, *J. Phys. Chem. C*, 2012, **116**, 23906–23914.

100 S. Y. Bang, M. J. Ko, K. Kim, J. H. Kim, I.-H. Jang and N.-G. Park, *Synth. Met.*, 2012, **162**, 1503–1507.

101 L. Han, A. Islam, H. Chen, C. Malapaka, B. Chiranjeevi, S. Zhang, X. Yang and M. Yanagida, *Energy Environ. Sci.*, 2012, **5**, 6057-6060.

 This journal is © The Royal Society of Chemistry 20xx

Please do not adjust margins

Please do not adjust margins

102 G. de Miguel, M. Marchena, M. Ziółek, S. S. Pandey, S. Hayase and A. Douhal, *J. Phys. Chem. C*, 2012, **116**, 12137–12148.

103 A. Morandeira, I. López-Duarte, B. O'Regan, M. V. Martínez-Díaz, A. Forneli, E. Palomares, T. Torres and J. R. Durrant, *J. Mater. Chem.*, 2009, **19**, 5016-5026.

104 S. M. Shah, Z. Iqbal, M. Iqbal, N. Shahzad, A. Hana, H. Hussain and M. Raheel, *Aust. J. Chem.*, 2014, **67**, 819–825.

105 N. A. Treat, F. J. Knorr and J. L. McHale, *J. Phys. Chem. C*, 2016, **120**, 9122–9131.

106 Asdim, K. Ichinose, T. Inomata, H. Masuda and T. Yoshida, *J. Photochem. Photobiol. A Chem.*, 2012, **242**, 67–71.

107 A. C. Khazraji, S. Hotchandani, S. Das and P. V. Kamat, *J. Phys. Chem. B*, 1999, **103**, 4693–4700.

108 S. Gadde, E. K. Batchelor, J. P. Weiss, Y. Ling and A. E. Kaifer, *J. Am. Chem. Soc.*, 2008, **130**, 17114–17119.

109 S. Gadde, E. K. Batchelor and A. E. Kaifer, *Chem. - Eur. J.*, 2009, **15**, 6025–6031.

110 A. Mishra, M. K. R. Fischer and P. Bäuerle, *Angew. Chem. Int. Ed.*, 2009, **48**, 2474–2499.

111 K. Gräf, M. A. Rahim, S. Das and M. Thelakkat, *Dyes Pigm.*, 2013, **99**, 1101–1106.

112 C. H. Lee, S. A. Kim, M. R. Jung, K.-S. Ahn, Y. S. Han and J. H. Kim, *Jpn. J. Appl. Phys.*, 2014, **53**, 08NC04.

113 G. Pepe, J. M. Cole, P. G. Waddell and S. McKechnie, *Mol. Syst. Des. Eng.*, 2016, **1**, 86–98.

114 G. Pepe, J. M. Cole, P. G. Waddell and J. R. D. Griffiths, *Mol. Syst. Des. Eng.*, 2016, **1**, 402–415.

115 B. E. Hardin, A. Sellinger, T. Moehl, R. Humphry-Baker, J.-E. Moser, P. Wang, S. M. Zakeeruddin, M. Grätzel and M. D. McGehee, *J. Am. Chem. Soc.*, 2011, **133**, 10662–10667.

116 B. E. Hardin, E. T. Hoke, P. B. Armstrong, J.-H. Yum, P. Comte, T. Torres, J. M. J. Fréchet, M. K. Nazeeruddin, M. Grätzel and M. D. McGehee, *Nat. Photonics*, 2009, **3**, 406–411.

117 J.-H. Yum, B. E. Hardin, E. T. Hoke, E. Baranoff, S. M. Zakeeruddin, M. K. Nazeeruddin, T. Torres, M. D. McGehee and M. Grätzel, *ChemPhysChem*, 2011, **12**, 657–661.

118 C. Siegers, U. Würfel, M. Zistler, H. Gores, J. Hohl-Ebinger, A. Hinsch and R. Haag, *ChemPhysChem*, 2008, **9**, 793–798.

119 H.-J. Son, C. H. Kim, D. W. Kim, N. C. Jeong, C. Prasittichai, L. Luo, J. Wu, O. K. Farha, M. R. Wasielewski and J. T. Hupp, *ACS Appl. Mater. Interfaces*, 2015, **7**, 5150–5159.

120 H.-J. Son, C. Prasittichai, J. E. Mondloch, L. Luo, J. Wu, D. W. Kim, O. K. Farha and J. T. Hupp, *J. Am. Chem. Soc.*, 2013, **135**, 11529–11532.

121 K. Hara, Y. Dan-oh, C. Kasada, Y. Ohga, A. Shinpo, S. Suga, K. Sayama and H. Arakawa, *Langmuir*, 2004, **20**, 4205–4210.

122 S. Buhbut, J. N. Clifford, M. Kosa, A. Y. Anderson, M. Shalom, D. T. Major, E. Palomares and A. Zaban, *Energy Environ. Sci.*, 2013, **6**, 3046-3053.

123 F. C. Spano, *Acc. Chem. Res.*, 2010, **43**, 429–439.

124 M. K. Brennaman, R. J. Dillon, L. Alibabaei, M. K. Gish, C. J. Dares, D. L. Ashford, R. L. House, G. J. Meyer, J. M. Papanikolas and T. J. Meyer, *J. Am. Chem. Soc.*, 2016, **138**, 13085–13102.

125 G. Chen, H. Sasabe, W. Lu, X.-F. Wang, J. Kido, Z. Hong and Y. Yang, *J. Mater. Chem. C*, 2013, **1**, 6547–6552.

126 Y. Li, Z. Li, Y. Wang, A. Compaan, T. Ren and W.-J. Dong, *Energy Environ. Sci.*, 2013, **6**, 2907–2911.

127 E. G. McRae and M. Kasha, *J. Chem. Phys.*, 1958, **28**, 721–722.

128 Y. Sun, Z. Liu, X. Liang, J. Fan and Q. Han, *Spectrochim. Acta Part A Mol. Biomol. Spectrosc.*, 2013, **108**, 8–13.

129 S. Kim, H. E. Pudavar, A. Bonoiu and P. N. Prasad, *Adv. Mater.*, 2007, **19**, 3791–3795.

130 V. Lau and B. Heyne, *Chem. Commun.*, 2010, **46**, 3595–3597.

131 H. Langhals, R. Ismael and O. Yürük, *Tetrahedron*, 2000, **56**, 5435–5441.

132 M. Pizzotti, F. Tessore, A. O. Biroli, R. Ugo, F. De Angelis, S. Fantacci, A. Sgamellotti, D. Zuccaccia and A. Macchioni, *J. Phys. Chem. C*, 2009, **113**, 11131–11141.

133 F. Nunzi, S. Fantacci, F. De Angelis, A. Sgamellotti, E. Cariati, R. Ugo and P. Macchi, *J. Phys. Chem. C*, 2008, **112**, 1213–1226.

134 D. Li, H. Wang, J. Kan, W. Lu, Y. Chen and J. Jiang, *Org. Electron.*, 2013, **14**, 2582–2589.

135 S. Kim, T. K. An, J. Chen, I. Kang, S. H. Kang, D. S. Chung, C. E. Park, Y.-H. Kim and S.-K. Kwon, *Adv. Funct. Mater.*, 2011, **21**, 1616–1623.

136 K. Westermark, H. Rensmo, H. Siegbahn, K. Keis, A. Hagfeldt, L. Ojamae and P. Persson, *J. Phys. Chem. B*, 2002, 106 (39), 10102–10107.

137 K. Keis, J. Lindgren, S. Lindquist and A. Hagfeldt, *Langmuir*, 2000, **16** (10), 4688–4694.

138 Y. Sakuragi, X. F. Wang, H. Miura, M. Matsui and T. Yoshida, *J. Photochem. Photobiol. A Chem*. 2010, **216** (1), 1–7.

139 M. Planells, A. Forneli, E. Martinez-Ferrero, A. Sanchez-Diaz, M. A. Sarmentero, P. Ballester, E. Palomares and B. C. O'Regan, *Appl. Phys. Lett.* 2008, **92** (15), 153506-(1-3).

140 A. B. Nepomnyashchii and B. A. Parkinson, *Langmuir*, 2013, **29**, 9362-9368.

141 C. S. Kley, C. Dette, G. Rinke, C. E. Patrick, J. Čechal, S. J. Jung, M. Baur, M. Dürr, S. Rauschenbach, F. Giustino, S. Stepanow and K. Kern, *Nano Lett.* 2014, **14** (2), 563–569.

142 J. M. Cole, M. A. Blood-Forsythe, T-C. Lin, P. Pattison, P. G. Waddell, L. Zhang, N. Koumura and S. Mori, *ACS Appl. Mater. Interfaces*, 2017, **9**, 25952-25961.

143 X. Liu, J. M. Cole, P. G. Waddell, T-C. Lin and S. McKechnie, *J. Phys. Chem. C*, 2013, **117**, 14130-14141.

144 J. M. Cole, K. S. Low, Y. Gong, *ACS Appl. Mater. Interfaces*, 2015, **7**, 27646−27653.

145 K. S. Low, J. M. Cole, X. Zhou, N. Yufa, *Acta Crystallogr. B*, 2012, **B68**, 137-149.

146 M. J. Griffith, M. James, G. Triani, P. Wagner, G. G. Wallace and D. L. Officer, *Langmuir*, 2011, **27**, 12944-12950.

147 J. McCree-Grey, J. M. Cole, S. A. Holt, P. J. Evans and Y. Gong, *Nanoscale*, 2017, **9**, 11793-11805.

Please do not adjust margins